*Revised Manuscript with no changes marked

On the sensitivity of modelled groundwater recharge estimates to rain gauge network scale

Andrew J. Wiebe* and David L. Rudolph

Department of Earth and Environmental Sciences, University of Waterloo, 200 University Avenue West, Waterloo, Ontario, N2L 3G1, Canada

* Corresponding author: Tel. +1 519 888 4567

E-mail addresses: ajwiebe@uwaterloo.ca (A.J. Wiebe), drudolph@uwaterloo.ca (D.L. Rudolph)

Abstract

Rainfall is often the largest component of the water budget and even a small uncertainty percentage may lead to challenges for accurately estimating groundwater recharge as a calculated residual within a water budget approach. Watersheds are a common scale for water budget assessment, and rainfall monitoring networks typically have widely spaced gauges that are frequently outside the watershed of interest. The effects of rainfall spatial variability and uncertainty on groundwater recharge estimates have received little attention and may influence water budget-derived recharge estimations. In the present study, the influence of spatial density in rainfall measurement on the numerical estimation of groundwater recharge was investigated through a series of modelling scenarios utilizing field data obtained from progressively denser rain gauge networks associated with a typical watershed in southern Ontario. The uncertainty of the recharge component of the water budget was used as a metric to aid interpretation of results. The scenarios employed networks composed of: 1) one nearby national weather station (within 3 km), 2) a regional network of six stations (within 30 km), and 3) a local network of six stations, five of which were within the selected watershed. A coupled and fully distributed hydrologic model (MIKE SHE) was used in the scenario analysis and applied to the Alder Creek watershed on the Waterloo Moraine near Kitchener-Waterloo, Ontario. Rainfall showed poor spatial correlation, even at the daily time scale. Average annual results over a three-year period showed that recharge rates varied up to 140 mm per year (~40 % of previously estimated annual recharge) among scenarios, with differences between scenarios greater than the water budget uncertainty during one of the years. These findings suggest that the availability of local rainfall

measurements has the potential to influence the calibration of transient watershed hydrogeological models.

1.0 INTRODUCTION

The estimation of groundwater recharge is a challenging task at any scale of consideration. With the emergence of regional scale groundwater models, often applied at a watershed scale, the seasonality and spatial variability of recharge has become a hydrologic component of significant importance. This is particularly the case when considering its role as a forcing function in water budgets and contaminant transport processes. Recharge magnitude and distribution is frequently estimated by numerical models that employ a water balance approach, where the magnitude of the recharge is calculated as a residual of the other measured or estimated components of the overall water budget (Healy, 2010). The calculated recharge distributions are then used as boundary conditions in modelling exercises related to watershed-scale assessments of water resources, regional impacts of non-point source contaminants, and changing land-use impacts. The rainfall data that are required for the water budget estimations are often derived from local weather stations that vary in spatial proximity to the study area.

While the scales at which rainfall measurements are made are known to influence their spatial accuracy over regional scales, the impact of measurement density on the spatial distribution of calculated groundwater recharge rates has received little attention (Hess et al., 2016; Sapriza-Azuri et al., 2015; Villarini et al., 2008; Winter, 1981). In many environments, precipitation (P) tends to be the largest component of the water budget (Dingman, 2015). Thus, small percentage uncertainties associated with P will lead to large magnitudes of uncertainty for smaller components of the overall hydrologic flow system – such as groundwater recharge or discharge – that are often estimated as residuals of the total water budget (Thodal, 1997; Wiebe et al., 2015; Winter, 1981). The optimal measurement scale required for rainfall measurements to ensure a particular degree of confidence in the estimation of groundwater recharge for a particular area is largely unknown and dependant on local conditions.

Many studies focused on the spatial variation of rainfall and the uncertainty associated with a particular network density have been undertaken to illustrate the significance of precipitation measurement (e.g., Dingman, 2015; Hess et al., 2016; Huff, 1970; Huff and Schickedanz, 1972; Linsley and Kohler, 1951; Villarini et al., 2008; Winter, 1981). The impact of spatial rainfall variability on streamflow has also been addressed, and it is well known that the number of rain gauges and their locations impact the accuracy of modelled hydrographs (e.g., Andréassian et al., 2001; Bell and Moore, 2000; Faurès et al., 1995; Obled et al., 1994; Zhao et al., 2013). Villarini et al. (2008) found that spatial correlation among rain gauges tends to increase, and spatial sampling errors tend to decrease, for increasing data accumulation times (e.g., 15 min, hourly, and daily). The authors do note, however, that the transferability of specific rainfall uncertainty results to other areas may not be directly applicable due to local site conditions.

Previous numerical studies addressing the influence of spatial rainfall variability on recharge have identified that interpolation techniques and the model's spatial grid size are important factors. Mileham et al. (2008) used a semi-distributed, soil-water budget model for a humid, tropical watershed in Uganda (2,098 km^2) over 15 years and found that cumulative recharge estimates differed by a factor of about 1.5 between a scenario interpolating precipitation via Thiessen polygons and one using inverse distance weighting with 20 rain gauges. Sapriza-Azuri et al. (2015) used a fully distributed model with stochastic rainfall distributions generated from rain gauges at 151 weather stations and found that recharge estimates varied based on the scale of the interpolated rainfall data (2.5 km by 2.5 km, or 50 km by 50 km, or lumped over the entire 16,000 km^2 watershed). Applying rainfall at the smallest grid cell size over four decades resulted in 1.5 to 2 times the recharge estimated when rainfall was applied at the other two scales. Recommendations for both the spatial density of observation points and selection of grid sizes for model input are needed for other geographical contexts.

Precipitation is frequently measured by rain/snow gauge networks, and ground-based radar methods rely on these for calibration (e.g., Dingman, 2015). The density of Canada's rain gauge network is less than 1 gauge per stream watershed in southern Ontario, where watersheds are on average about 300 km^2 in size (Adam and Lettenmaier, 2003; OMNR, 2007; OMNRF, 2016). Extreme summer rainfall events in this area may occur over 100 km^2 (Paixao et al., 2015), and convective summer storms can be as small as 5 to 8 km^2 in size (Singh, 1992; Tsanis and Gad, 2001). Such events could easily evade detection by existing rain gauge networks, and these may become increasingly important due to climate change (Collins et al., 2013; Cubasch et al., 2001; Jyrkama and Sykes, 2007). This is a potential concern for groundwater recharge estimation under both long-term and event-based conditions. The sustainable management of integrated water supplies depends on accurate quantitative estimates derived from precipitation measurements. Accurate precipitation estimates are also essential for assessing regional-scale water quality vulnerability related both to non-point contaminants and local, extreme hydrologic, event-based conditions near critical receptors such as public supply wells (e.g., Christie et al., 2009; the May 2000 Walkerton tragedy – O'Connor, 2002).

The objective of the present study was to assess the spatial correlation among point rainfall measurements, and to explore the sensitivity of modelled recharge estimates to spatial variations in rainfall in the vicinity of a typical watershed in southern Ontario. The watershed selected for this study represents watersheds where municipal water sources rely on glacial moraine aquifers, and agricultural activities and urban expansion present challenges related to water quality and quantity. It was hypothesized that recharge estimates in scenarios employing different rainfall networks' interpolated data would differ to a degree that could significantly impact regional water management decisions. The uncertainty associated with the recharge component of a near-surface water budget was employed as a metric of significance. Differences in recharge between scenarios were assessed based on: 1) visual analysis of the spatial distributions of total recharge, 2) the frequency of cell-by-cell differences in modelled total recharge, and 3) changes in water budget components such as cumulative streamflow. Three different spatial scales of rain gauge networks were used for the assessment: i) one national station located within 3 km of the watershed, ii) six regional stations within 30 km of the watershed, and iii) six local stations, five of which were within the watershed. The sensitivity was addressed by comparing the magnitude and spatial distribution of recharge results from three corresponding scenarios: (1) spatially uniform rainfall from the national network, and spatially variable rainfall interpolated from the (2) regional and (3) local networks. Spatially uniform reference evapotranspiration (ET_o) derived from the national network station was used for all scenarios, and spatial variations in snowfall were held constant in order to isolate rainfall as the variable of comparison.

For this investigation, field data collected from the local rain gauge network within the study region over a three-year period were utilized to illustrate natural precipitation variability.

We specifically addressed this relatively short temporal period because this is the time scale at which fully-coupled models may be used in practice by environmental consultants to study the impacts of dynamic hydrological events on city water supply systems (Meyer et al., 2017). There could be different results over a longer time scale.

2.0 METHODS

2.1 SITE DESCRIPTION

The Alder Creek watershed (78 km^2; Figure 1) within the Grand River watershed (6,700 km^2) is located on the regional upland of the Waterloo Moraine (GRCA, 1998). Located adjacent to the cities of Kitchener and Waterloo, ON, this watershed's glacial sands and gravels cover over half of its surficial area and facilitate recharge for about seven municipal well fields operated by the Regional Municipality of Waterloo (Brouwers, 2007; CH2MHILL and SSPA, 2003; OGS, 2010). Due to its importance for water supply, the watershed and its surrounding area have been the subject of detailed hydrologic modelling in the past (e.g., CH2MHILL and SSPA, 2003; Martin and Frind, 1998; Matrix and SSPA, 2014a, 2014b; Sousa, Frind, et al., 2013). The availability of extensive subsurface geology data and hydrogeological interpretations derived from previous work in the area provides a valuable foundation for the current modelling exercises within the multi-aquifer system of the Waterloo Moraine (e.g., Bajc et al., 2014; Blackport et al., 2014; CH2MHILL & SSPA, 2003; Martin and Frind, 1998).

Total annual precipitation is around 900 mm in this region, varying between 600 and 1100 mm at the nearby Environment Canada weather station at Roseville, ON, which is located less than 3 km outside the watershed (Government of Canada, 2019; OMNR, 2007). Actual ET

(AET) for the region has been estimated at generally around 540 mm per year (Sanderson, 1998), and streamflow is on average around 140 mm per unit area at the gauging station within the watershed (Figure 1; based on daily data, 1975-2015; WSC, 2017). The average baseflow index (i.e., the fraction of total streamflow constituted by groundwater baseflow) for this station is about 0.6, according to quarter-year PART hydrograph separation results (based on daily data, 1966 to 2016; Rutledge, 2007; WSC, 2017).

National network daily precipitation and temperature data were obtained for the Roseville weather station noted above and shown in Figure 1 (Government of Canada, 2019); this is the closest national station to the Alder Creek watershed. Rainfall data were recorded using a Canadian Type B rain gauge (113 mm diameter) at a height of 0.4 m and available on a daily timescale, while snow depths were manually measured each day and converted to snow water equivalent using a ratio of 0.1 (Government of Canada, 2013, 2019). Daily maximum and minimum temperatures were obtained from the Roseville station for ET_o calculations.

Regional network rainfall data were obtained from six stations operated by the Grand River Conservation Authority (GRCA) and shown on the inset map of Figure 1. Rainfall data were available at an hourly time scale from a network of tipping-bucket gauges installed for the purposes of flood forecasting (GRCA, 2017a; Shifflett, pers. comm., 2018).

Local network rainfall data were obtained from the Alder Creek field observatory of the Southern Ontario Water Consortium (SOWC; Wiebe et al., 2019). This network of weather stations (Figure 1) employed tipping bucket rain gauges (200 mm diameter) recording data every 15 min. Each of the six gauges was installed at a height of 1 m above the ground surface and surrounded by an Alter-type wind shield. Data were available for January 2014 onward for all stations except WS5, where data records began in June 2014. Annual rainfall totals are shown in Table 1 for each of the three rain gauge networks.

2.2 SPATIAL CORRELATION

Spatial correlation for rainfall was assessed using Spearman's rank correlation coefficient for several accumulation times (Gibbons and Chakraborti, 1992; Villarini et al., 2008; Villarini et al., 2010). Each coefficient was generated by comparing the data from a pair of stations. For each accumulation time (1 hr, 3 hr, 24 hr, 1 month), the sum of the data within each time interval of that size was compared. Each correlation coefficient measures the strength of the linear relationship between ranked data at a pair of stations. The Spearman rank correlation coefficient was used instead of the Pearson coefficient because the Pearson method assumes that the data are normally distributed, while the Spearman coefficient does not (Gibbons and Chakraborti, 1992). Rainfall data were assessed for the combined stations of the local and regional networks. The overall time period for this correlation analysis was three years, except for correlations involving station WS5, which employed 2.5 years of data. An exponential model (Villarini et al., 2008) relating the correlation coefficient, ρ, to the separation distance, h, was employed to fit the data and show general trends in correlation for the different accumulation times (Eqn. 1):

$$\rho(h) = c_1 exp\left[-\left(\frac{h}{c_2}\right)^{c_3}\right]. \tag{1}$$

The parameters c_1, c_2, and c_3 represent the nugget, correlation distance, and shape factor, respectively (Villarini et al., 2008). Following Villarini et al. (2010) and based on arguments by

Krajewski et al. (2003) that a traditional network of rain gauges (one gauge per location) is insufficient to estimate c_1, a nugget value of c_1 = 1.0 was chosen in all cases. The correlation distance and shape factor for the field data were determined via the Levenberg-Marquardt algorithm in the scientific computation program GNU Octave (Eaton et al., 2011; Gavin, 2009, 2019).

2.3 WATER BUDGET AND UNCERTAINTY

Context for the recharge differences between scenarios was portrayed by calculating the uncertainty from an annual vadose zone water budget (Eqn. 2),

$$R = P - AET_{VZ} - Q_{SW} - \Delta S_{VZ}, \tag{2}$$

where R is recharge, P is total precipitation, AET_{VZ} is actual evapotranspiration from the vadose zone, Q_{SW} is the surface water fraction of streamflow (i.e., 1 – baseflow index), and ΔS_{VZ} is net storage change in the vadose zone. This water budget assumes that recharge occurring from surface water bodies directly connected to the water table is negligible, i.e., that all recharge migrates through the unsaturated zone. AET derived from the saturated zone is excluded from this water budget because the domain for this budget is the vadose zone; AET derived from the saturated zone has already become recharge (R) and thus should not be counted twice. Uncertainty on recharge (δR) was calculated under the assumption that the individual uncertainties are independent (e.g., Dingman, 2015) via (Eqn. 3),

$$\delta R = \sqrt{\delta P^2 + \delta AET^2 + \delta Q^2 + \delta \Delta S_{VZ}^2}, \tag{3}$$

where δP is precipitation uncertainty, (~10%, Dingman, 2015); δAET is AET uncertainty, (~10%, Kristensen and Jensen, 1975); δQ is streamflow uncertainty, (~5%, Herschy, 1973; Winter, 1981); and $\delta \Delta S_{VZ}$ is uncertainty related to vadose zone storage change, (~5%, assumed similar to streamflow). Spatial interpolation errors for P and AET were not included. The uncertainty of the water budget components in Eqn. (3) was calculated using the input data and results for a scenario and year with a percentage uncertainty on R that was similar to the average from all annual simulations, as an example of a typical case.

2.4 NUMERICAL MODEL

The fully distributed MIKE SHE software code (Abbott et al., 1986; Graham and Butts, 2005; Refsgaard and Storm, 1995) was used to conceptually explore the sensitivity of recharge estimates to spatial variations in rainfall. This code internally couples the saturated zone (3D), unsaturated zone (1D), overland flow (semi-distributed), and streamflow (1D) processes, with surface boundary inputs and outputs such as P and ET_o. The ground surface topography and seven geological layers for the model were imported from an existing three-dimensional groundwater flow model (Region of Waterloo Tier Three water budget and risk assessment; Matrix and SSPA, 2014a) and interpolated onto a grid with 50 m by 50 m cells that composed the domain for the present study. This included hydraulic conductivity values that had been calibrated for steady state conditions in the existing model, which used the finite element-based FEFLOW code (DHI-WASY, 2011). Hydraulic head values from the existing model were applied at the boundaries of the Alder Creek watershed and specified as the initial conditions within the domain. The boundary of the domain (Figure 1) was designed to coincide with the New Dundee dam at the outflow of Alder Lake, about 8 km upstream from the actual outflow of Alder Creek into the Nith River. This allowed for a well-defined hydraulic head boundary in the surface water portion of the model. The resulting model domain area was 68 km^2, and the revised boundaries adjacent to the dam followed local topographic ridges to the watershed divide (GRCA, 1998).

Precipitation inputs to the model were developed from daily national data, hourly regional data, and 15 min local rainfall data. Rainfall data for the regional and local scenarios were aggregated to the daily time scale and interpolated onto a 250 m by 250 m grid using the inverse distance squared technique. Rainfall data for the national scenario were applied at the daily time scale in a spatially uniform manner. All scenarios employed daily snowfall data from the Roseville station. The model used the average daily air temperature at the Roseville station to calculate the accumulation and melting of snow, based on a modified degree day method (DHI, 2017a; Government of Canada, 2019).

Drainage of water in the unsaturated zone was represented by the 1D Richards' Equation option (DHI, 2017a). Soil columns for each grid cell were composed of one single soil type corresponding to the surficial soil because the model framework did not allow automated incorporation of the detailed geological layering into the unsaturated zone. Each column was discretized with 0.1 m cells down to 10 m, then 0.2 m cells to 30 m, and then 1 m cells to 55 or 80 m depth. The spatial distribution of nine surficial soil types (Figure 2) was based on OGS (2010). Saturated hydraulic conductivity, porosity, and residual moisture content parameters for the van Genuchten curves were based on literature values (D. Graham, pers. comm., 2017; Schaap et al., 1999; Sousa, Jones, et al., 2013), and the n, alpha, and Green and Ampt suction at the wetting front parameters were selected in order to vary in a conceptually reasonable manner in comparison with the UNSODA soil types (D. Graham, pers. comm., 2017; Leij et al., 1996; Table 2). No macropore flow was simulated. The default pressure head values for field capacity and wilting point (-1 m H_2O, and -100 m H_2O, respectively), and the default shape factor for unsaturated hydraulic conductivity (0.5) were selected based on DHI (2017b) recommendations.

Daily ET_o inputs to the model were calculated based on the Penman-Monteith method for reference ET, using the UNFAO56 ET_o Calculator (Allen et al., 1998; Raes, 2009). The maximum and minimum daily temperatures at the Roseville station were used to calculate ET_o for all three scenarios. The "light to moderate winds" option (2 m/s at a height of 2 m above ground surface) was selected to fill in missing wind speed data in the ET_o calculations.

The upper three geological layers that were imported from the existing model were merged into one computational layer for the saturated zone simulation. This ensured that the water table would be present in the uppermost saturated zone cell, improving the stability of the model. The minimum geological layer thickness was set to match the input layers from the existing model (0.1 m). The finite difference option was used to represent flow in the saturated zone (DHI 2017a). Public supply wells within the watershed were incorporated into the model and their average 2008 pumping rates were employed (total extraction: 23,000 m^3/d; Matrix and SSPA, 2014b).

Land use and vegetation data (Figure 3) were compiled from ROW (2010) and from the Ontario Ministry of Natural Resources (OMNR, 2008). The sparse paved areas were not treated specially beyond maintaining an assigned background rooting depth, as required by the model, though the urban areas were assigned a leaf area index (LAI) value representing grass. Maximum

LAI and root depths were obtained from the literature (Canadell et al., 1996; Scurlock et al., 2001). The LAI values for agricultural areas were assigned a linear increase from zero up to the respective literature value for each cell during the month of May; rooting depths linearly increased during the growing season (May to mid-September). LAI was specified to linearly increase for forest areas during May, be held constant during the growing season, and then linearly decrease during the last two weeks of September. No irrigation was included in the model.

Overland flow was represented using a semi-distributed approach via the finite difference method (DHI 2017a). A Manning's *n* value of 0.3 $m^{-1/3}s$ was applied throughout the domain to represent the majority agricultural land use with a value for light brush, and detention storage was specified based on literature values for five of the land cover types (Chin, 2006), excluding wetlands and open water.

Stream channels were generated based on the pre-processed (interpolated) model topography to obtain more reasonable agreement between the streamflow and overland flow processes, and cross-sections were generated every 200 m. Manning's *n* values for the channel were based on GRCA (2017b): 0.035 $m^{-1/3}s$ for the channel thalweg, and 0.05 $m^{-1/3}s$ otherwise.

The model employs independent, automatically adjusted time steps for its overland flow, unsaturated zone, and saturated zone processes (DHI, 2017c; Graham and Butts, 2005). Groundwater recharge is calculated iteratively as an internal flux from the unsaturated zone to the saturated zone during simulations (Graham and Butts, 2005); the accumulated amount for a single cell or the entire watershed was obtained via post-processing.

2.5 COMPARISON OF MODEL SIMULATIONS

The scenarios were simulated one year at a time for the years 2014 to 2016. The 2014 simulations followed a three-year model spin-up period that employed spatially uniform daily rainfall and snowfall data from the Roseville station. Scenarios 2 and 3 were started from the same initial conditions as Scenario 1 in all three years. The method of comparing simulations with different rainfall inputs that start from identical initial conditions has been used in other studies (e.g., Schuurmans and Bierkens, 2007; Sapriza-Azuri et al., 2015). Our study differs from Schuurmans and Bierkens (2007) by focusing on groundwater recharge rather than hydraulic heads and discharge, and from Sapriza-Azuri et al. (2015) by addressing a much smaller watershed (~70 km^2 vs. 16,000 km^2) using rainfall interpolated from observations within different networks rather than stochastic values derived from the overall network. Results from the numerical model were saved on a weekly basis, so each year was represented by 52 weeks during analysis of the simulations. The results were compared based on maps of the spatial distribution of total recharge, the frequency of cell-by-cell differences in total recharge, the visual match between observed and modelled cumulative streamflow, and differences in overall water budget components.

None of the three simulations were calibrated. This study compared the impacts of the different rainfall input data on the precision of the estimated recharge distributions. Each set of input data would result in a different calibrated model, but modifications to the parameters of the model (e.g., hydraulic conductivity values) would obscure the effects of the input data on recharge rates. Using the same starting point for each 52-week simulation allows the differences in recharge rates to be compared for a model domain structure that is identical in all cases (i.e., the same set of hydraulic conductivity values for the geological layers). The comparison of modelled streamflow for each scenario provides a sense of the degree of calibration that would be required.

Observed and simulated rainfall amounts were compared as follows. The spatial correlation of the numerical model's interpolated rainfall datasets was assessed by selecting 36 uniformly spaced cells from the grid, extracting their precipitation time series, and calculating Spearman correlation coefficients for days with no Roseville snowfall. Days with snowfall were omitted because the observed and simulated daily snowfall amounts differed slightly due to the model's partitioning of rain and snow based on temperature. Rainfall frequency distributions for these 36 cells were also compared with the observed distributions.

3.0 RESULTS

The spatial correlation of rainfall was found to vary substantially at both the regional and local scales. Figure 4 suggests a continuum in the spatial correlation relationships as distance increases from the local to the regional scale. Daily Spearman correlation coefficients ranged between approximately 0.4 and 0.8 (Figure 4). Correlation distances and shape factors for the combined stations of the local and regional networks are shown in Table 3 for different time scales. Correlation distances associated with the fitted curves on Figure 4 ranged from about 90 to 110 km. The best-fit curve for monthly coefficients showed lower correlation than the daily curve. Correlation coefficients in the local network were substantially lower than those reported for a dense monitoring network (50 gauges in 135 km^2, 6 years of data) in the Brue Watershed, SW England (Villarini et al., 2008). Daily (Pearson) coefficients were ≥ 0.85 in that study, while these varied between roughly 0.6 and 0.9 for the local network in the present study. The spatial correlation analysis indicates that: 1) rainfall may not be sufficiently uniform temporally and spatially in the region around Alder Creek to justify either reliance upon a single rain gauge to represent the watershed or the neglect of rainfall variation within the watershed itself, and 2) the local network is providing additional rainfall information not captured by the regional network.

The inverse distance squared interpolation technique was found to increase the spatial correlation of the interpolated daily precipitation distributions for the regional and local rainfall scenarios. All Spearman cofficients among 36 uniformly spaced sample points for both Scenarios 2 and 3 were between 0.7 and 1.0, a higher range than observed. Appendix A includes examples of the rainfall interpolation for four representative days with a range of rainfall rates. The interpolated daily rainfall frequency distributions at these 36 points for Scenarios 2 and 3 were similar to those observed within the local and regional networks (Appendix A).

A simple, annual water budget for the vadose zone provided a metric for the differences in recharge between scenarios. Figure 5 shows that typical instrument and method uncertainty values on these components lead to a substantial accumulated percentage uncertainty on recharge (±27%), prior to accounting for spatial interpolation uncertainties for P or ET. The uncertainty on recharge (δR) could be at least ±100 mm per year (using Scenario 3 data for 2015; Table 4), with precipitation measurement uncertainty as the largest contributor. Analysis of error for small groundwater components is often disregarded when conducting calibration and water budget uncertainty estimations (Wiebe et al., 2015).

The water budget results from the three scenarios are listed in Table 4, along with other relevant values for the watershed: the observed streamflow totals from the WSC gauge, and a regional, steady state model's estimate of average recharge (M.H. Brouwers, pers. comm., 2017; Matrix and SSPA, 2014a; WSC, 2017). The average total precipitation driving the water budget in the numerical model was different in each of the three rainfall scenarios, and the direction of change from year to year sometimes differed. Table 4 shows that average total precipitation increased from 2015 to 2016 in both Scenarios 1 and 2, while it decreased for Scenario 3. Precipitation differences between scenarios for a given year were up to about ±20% of the long-term average from Roseville. Differences in average recharge varied up to around 140 mm per year, or 44% of average steady state recharge (321 mm; M.H. Brouwers, pers. comm., 2017; Matrix and SSPA, 2014a), although Scenarios 1 and 3 showed nearly equivalent average recharge for 2016. Differences in average recharge with respect to Scenario 3 were greater than the magnitude of the water budget δR for both comparisons in 2014, and for the comparison with Scenario 2 in 2015. Vadose zone AET rates were similar (within ±11 mm of Scenario 3) in 2014 and 2015; AET for Scenarios 1 and 2 differed from Scenario 3 by +106 mm or +44 mm in 2016, respectively, despite having identical ET_o input values. This shows a "cascade" effect of the variation of rainfall on other water budget parameters calculated by the numerical model: Differing rainfall inputs can influence AET rates which in turn influence recharge rates. Figure 6 shows the spatial distribution of recharge rates for the three rainfall scenarios. Net groundwater discharge conditions are generally present along the Alder Creek channel and tributaries. The 2014 maps (a, d, and g) show similar recharge distributions for Scenarios 1 and 2, and higher recharge rates everywhere except near the stream channels for Scenario 3. The 2015 maps (b, e, and h) particularly show differences in recharge rates between different scenarios in the sand and gravel soil types. The 2016 maps (c, f, and i) show similar spatial recharge patterns for Scenario 1 and Scenario 3 and lower recharge for Scenario 2, reflecting the lower precipitation in Scenario

2 (Table 4). While general spatial differences in recharge rates may be observed in the Figure 6 information, Figure 7 presents the frequency of cell by cell differences between scenarios. Despite the similar overall average recharge in the local and national rainfall scenarios in 2016 (Table 4), the frequency plot (Figure 7c) shows that this is the result of a balancing of increases and decreases in recharge across the domain. Comparisons involving the local rainfall scenario produced a broader distribution of cell by cell differences in recharge, while the differences between the regional and national scenarios resulted in a more general shift that affected more cells similarly. That is, a greater number of cells changed by differing amounts of recharge when the local rainfall scenario was compared with either of the other two rainfall scenarios.

Figure 8 shows that the cumulative streamflow results for the scenario employing local rainfall were closer to the observed streamflow in all three years simulated. Scenario 3 streamflow was about 3% lower than the observed cumulative flow at the WSC gauge at the end of 2014, about 10% lower at the end of 2015, and about 20% lower at the end of 2016. Cumulative streamflow results from Scenario 1 were between 25 and 31% lower during the three years, whereas Scenario 2 results were between 27 and 43% lower. Because Scenario 3 provided closer agreement with recorded values in all three years, the local rainfall scenario could be interpreted as requiring less extensive calibration than the other two. However, the baseflow indices at the node representing the WSC gauge were between 0.21 and 0.31 for all scenarios. Scenario 3 had the lowest baseflow values. The model predicted a larger overland flow component of streamflow and much lower baseflow than observed (~0.6; Rutledge, 2007; WSC, 2017).

Overall, the poor spatial correlation in rainfall near the study area resulted in differences in recharge rate estimates for 2014 to 2016 that were largest when the local rainfall scenario was compared with either the regional or national network scenarios. Local rainfall interpolations generally led to recharge and streamflow results that were markedly different than those associated with rainfall from the regional or national networks, suggesting a high degree of sensitivity of recharge rates to the scale of rainfall input data.

4.0 DISCUSSION

The results suggest that recharge distributions estimated through numerical modeling can be quite sensitive to the spatial variability of rainfall, as characterized by the spatial correlation analysis. While longer term monitoring followed by modelling would provide a more complete evaluation of the issue, this study suggests that the significant investment required for that research would likely produce non-trivial differences in modelled recharge rates for watersheds similar to Alder Creek for some years. Annual recharge rates could differ by a considerable percentage of the average long-term recharge (e.g., 40%). Local rainfall measurements are frequently unavailable at the scale of watersheds used for public water supply, yet models are frequently used for water management at this scale and in similar settings. The implications of the results are discussed below, following discussion of several aspects of the study itself.

The four main factors that could have influenced the recharge results of this study are: 1) the uncertainty associated with measured rainfall amounts, 2) the frequency of applied rainfall intensities in the model, 3) the increased correlation of rainfall caused by the interpolation method, and 4) the rainfall regimes sampled by the short-term monitoring of the local rainfall network (3 years). First, the accuracy of the readings at the individual rain gauges could influence the interpolated rainfall distribution applied to the model, and therefore recharge. All rainfall measurements are susceptible to human and instrument errors. The local network rain gauges were observed to have instrument errors up to ±10% on average when tested. The wind screens around the local network's gauges reduce the degree to which wind effects are expected to bias the data, while the regional network likely has a higher level of uncertainty due to infrequent calibration and a typical lack of wind screens. The daily volumetric capture of the Roseville rain gauge was likely to be measured quite accurately, though the wind effects would be different because the gauge type differs from the other two networks.

Second, Mileham et al. (2008) found that the frequencies of interpolated daily rainfall amounts impacted recharge rate estimates. In contrast to the Mileham et al. (2008) study, interpolated daily frequencies of rainfall amounts for the regional and local rainfall scenarios in the present study were similar to each other and to the frequencies observed at the local rain gauges (Appendix A). The lack of noteworthy frequency differences between the interpolated and measured amounts suggests that variations in the rainfall frequency distribution are not a major factor.

Third, recharge rates could have been influenced by the increased spatial correlation of rainfall caused by the inverse distance squared interpolation technique. Interpolation shifted the entire range of Spearman correlation coefficients upward by about 0.2, from about 0.4 to 0.8 for the observed rainfall to about 0.7 to 1.0 for the simulated. Two related issues are: 1) software packages used for fully distributed watershed modelling typically restrict the user to the choice of a small number of interpolation methods, and 2) a more advanced method such as kriging may require a larger number of observation points than are frequently available.

Fourth, the short-term nature of data collected by the local rain gauge network may have biased the recharge results by limiting the period of analysis to three years. Thus, the concern is that the limited analysis may not be representative of the actual long-term data. However, the dataset does include two of the types of years that would be desirable in a more extensive study: the rainfall at Roseville in 2016 was essentially equal to the long-term average rainfall over 1973 to 2018, and the rainfall in 2014 and 2015 was lower than average (by about 12 and 9%, respectively). Though the recharge modelling is missing a comparative, higher than average rainfall amount for Roseville, the results do suggest that drier years (at the national station) may be more interesting in terms of greater variability in rainfall and recharge (Table 4). While modelling longer-term impacts of the choice of rain gauge measurement network on recharge variability would be preferable, the purpose of present study was to conduct an initial assessment and suggest whether investments in local rainfall monitoring might improve confidence in groundwater recharge estimates.

The results of this study have implications for the calibration of hydrogeological models, and therefore implications for the delineation of wellhead protection areas (capture zones), the estimation of groundwater contribution areas for stream reaches, the quantification of the groundwater volume available for long-term extraction, and the assessment of contaminant loadings and transport. The results also provide advice on hydrological monitoring investments. While boundary conditions such as spatial variation in rainfall rates could be estimated during the calibration process (e.g., Anderson and Woessner, 1992), it is common in practice to apply whatever precipitation data are available to fully distributed models and focus calibration efforts on modifying hydraulic conductivity values in order to match observed hydraulic heads and streamflow (Kampf and Burges, 2010). This is a potential concern. In either transient or steady state calibration, a lack of precision in the rainfall distribution will be compensated for by adjustments of the hydraulic conductivity and other soil parameters, potentially mis-representing the actual geology and biasing infiltration and drainage rates. Steady state models would be unable to incorporate repeating rainfall patterns that may exist at small scales without being captured by existing national networks. Such patterns could be caused by trends in wind direction and rainfall distributions associated with evaporation from large lakes (Dingman, 2015) or a heat-island effect near cities (Renard, 2017). The sustainable management of groundwater resources could be impaired by water budget errors related to the precision of rainfall data. For instance, a recharge uncertainty of ±100 mm (Figure 5) over the 68 km^2 model domain in the present study is roughly equivalent to ±50% of the adjacent City of Kitchener's (population ~ 230,000) annual groundwater extraction (Matrix and SSPA, 2014b).

The magnitude and spatial distribution of recharge is a significant uncertainty for steady state capture zone delineation (Sousa, Frind, et al., 2013). This would be further pronounced for transient capture zones (e.g., Graham and Butts, 2005). Precise rainfall measurements could also affect the recharge rates used to delineate areas of groundwater contribution for stream reaches, which could be an important aspect of land use planning and low impact development strategies aimed at maintaining baseflow to streams (e.g., Chow et al., 2016).

Contaminant loadings and transport depend on accurate recharge rates. Recharge distributions also affect the flowpaths of contaminants to receptors such as wells and wetlands and their associated reaction potential (e.g., Loschko et al., 2016). In addition to the potential amount of dilution experienced by contaminants based on recharge rate variation due to the rainfall input data employed, the estimation of dispersion coefficients could also be affected (Yin et al., 2015). Factors such as rainfall amounts, timing, and intensity that could influence recharge rates have been found to influence pesticide leaching rates in the vadose zone (Isensee and Sadeghi, 1995; Sadeghi and Isensee, 1994).

Spatial correlation information for rainfall could be used to enhance groundwater modelling. Correlation statistics could guide the design of rainfall monitoring networks used to collect model input data. Comparison of the spatial correlation coefficients for rainfall in the Brue watershed (Villarini et al., 2008) and the Alder Creek watershed suggests that Alder Creek requires relatively more rainfall observation points to capture the spatial variability over small distances (< 15 km). Correlation could also be used to interpret how well sparse rainfall observation stations represent an area, or discrepancies between sparse rainfall data and water table responses.

While long-term, high quality records at national weather stations such as Roseville are invaluable, watershed studies at shorter time-scales (transient as opposed to steady state) in certain regions are likely to benefit from more spatially precise rainfall data. The results of the present study suggest that the scale of available data could bias hydraulic conductivity values as calibration compensates for a lack of precise rainfall observations, thus mis-representing recharge and discharge in the near-surface environment. Increasing the density of rain gauges may also be the most cost-effective way to reduce uncertainty associated with recharge estimates, when compared with the cost of collection of subsurface information at the point scale, such as drilling more wells, analyzing soil samples, and conducting hydraulic tests.

5.0 CONCLUSIONS

The results of this study indicate that rain gauge network scale can have a significant impact on recharge rate estimates at the watershed scale during short (annual) time scales. Daily Spearman spatial correlation coefficients between gauges of the local and regional networks were typically < 0.8. These correlations show that rainfall is not uniform in the vicinity of the Alder Creek watershed. Simulation of the three rainfall networks resulted in differences in overall average recharge of up to 140 mm, or around 40% of previously estimated steady state recharge (M.H. Brouwers, pers. comm., 2017; Matrix and SSPA, 2014a). Differences in recharge rates between the scenario employing local rainfall and each of the other two rainfall scenarios were more variable than comparisons between the national and regional scenarios, and cumulative streamflow for the local rainfall scenario visually appeared to provide a closer match with observed streamflow. The overall conclusion is that in a setting such as the one described by the observed ranges of local and regional spatial rainfall correlation coefficients, fully distributed, transient models may frequently be compensating for actual rainfall inputs via adjustment of hydraulic conductivity values during calibration. This is a concern for land use planning with the goal of maintaining baseflow to streams, for long-term water resources projections, for representing transient hydrological events, and for contaminant transport models that rely on accurate recharge rate estimates.

Future work should address the impact of radar rainfall data and snowfall distributions on recharge estimates at the watershed scale.

ACKNOWLEDGEMENTS

We acknowledge the support of the Natural Sciences and Engineering Research Council of Canada (NSERC) in this collaboration between the University of Waterloo and Matrix Solutions Inc. (IPS Grant #485430 to the first author; Discovery Grant to the second author). The authors are grateful to the individuals and businesses who hosted the weather stations: R. and W. Goettling, Rebel Creek Golf Club, G. and L. Kaster, Region of Waterloo, Herrle's Country Farm Market, D. and P. Mighton, and Nith Valley Organics. Paul Martin and Steve Murray provided valuable advice and assistance during the modelling process, and Gaelen Merritt assisted with the van Genuchten parameters. Thanks to Sage McKay, James Elliott, Jack Robertson, Emilie Mesec, Paul Menkveld, Ian Mercer, Kristen Blowes, Elliot Pai, Elton Huang, Sarah Indris, and technician Paul Johnson for assistance with field equipment setup and maintenance, testing the accuracy of rain gauges, and compiling data. Brewster Conant, Jr., James Craig, and Philippe Van Cappellen provided helpful suggestions. Thanks to Christopher Neville, Brittney Glass, Maria Giovanna Tanda, Gonzalo Sapriza-Azuri, and two anonymous reviewers for reviewing previous versions of the manuscript. Field equipment was provided by the Southern Ontario Water Consortium (FedDev Ontario; Ontario MEDI).

APPENDIX A

One supplementary information file contains: a brief description of one additional model scenario, examples of the interpolated rainfall distributions, and a comparison of observed and modelled rainfall frequency distributions.

REFERENCES

Abbott, M.B., Bathurst, J.C., Cunge, J.A., O'Connell, P.E., Rasmussen, J., 1986. An introduction to the European Hydrological System-Système Hydrologique Européen, SHE, 2: Structure of a physically-based, distributed modelling system. J. Hydrol. 87, 61-77. https://doi.org/10.1016/0022-1694(86)90115-0.

Adam, J.C., Lettenmaier, D.P., 2003. Adjustment of global gridded precipitation for systematic bias. J. Geophys. Res. 108(D9), 4257. https://doi.org/10.1029/2002JD002499.

Allen, R.G., Pereira, L.S., Raes, D., Smith, M., 1998. Crop evapotranspiration – Guidelines for computing crop water requirements – FAO Irrigation and drainage paper. FAO (Food and Agriculture Organization of the United Nations), Rome, IT. http://www.fao.org/docrep/X0490E/X0490E00.htm. (Accessed 05.05.2017).

Anderson, M.P., Woessner, W.W., 1992. Applied Groundwater Modeling: Simulation of Flow and Advective Transport. Academic Press, San Diego, CA, USA.

Andréassian, V., Perrin, C., Michel, C., Usart-Sanchez, I., Lavabre, J., 2001. Impact of imperfect rainfall knowledge on the efficiency and the parameters of watershed models. J. Hydrol. 250, 206-233. https://doi.org/10.1016/S0022-1694(01)00437-1.

Bajc, A.F., Russell, H.A.J., Sharpe, D.R., 2014. A three-dimensional hydrostratigraphic model of the Waterloo Moraine area, southern Ontario, Canada. Can. Water Resour. J. 39(2), 95-119. https://doi.org/10.1080/07011784.2014.914794.

Bell, V.A., Moore, R.J., 2000. The sensitivity of catchment runoff models to rainfall data at different spatial scales. Hydrol. Earth System Sci 4(4), 653-667. https://doi.org/10.5194/hess-4-653-2000.

Blackport, R.J., Meyer, P.A., Martin, P.J., 2014. Toward an understanding of the Waterloo Moraine hydrogeology. Can. Water Resour. J. 39(2), 120-135. https://doi.org/10.1080/07011784.2014.914795.

Brouwers, M.H., 2007. A case study for assessing the hydrologic impacts of climate change at the watershed scale. Unpublished MASc. Thesis, University of Waterloo, Waterloo, ON, Canada. 121p. http://hdl.handle.net/10012/3514.

Brouwers, M.H., 2017. Personal communications from groundwater modelling specialist at Matrix Solutions Inc. Tier Three recharge results shapefile exported from FEFLOW, Sim836 (Sim836_Rch.shp).

Canadell, J., Jackson, R.B., Ehleringer, J.R., Mooney, H.A., Sala, O.E., Schulze, E.-D., 1996. Maximum rooting depth of vegetation types at the global scale. Oecologia 108, 583-595. https://doi.org/10.1007/BF00329030.

Chin, D.A., 2006. Water-Resources Engineering. 2nd Ed. Pearson Prentice Hall, Upper Saddle River, NJ, USA.

Chow, R., Frind, M.E., Frind, E.O., Jones, J.P., Sousa, M.R., Rudolph, D.L., Molson, J.W., Nowak, W., 2016. Delineating baseflow contribution areas for streams – A model and methods comparison. J. Contam. Hydrol. 195, 11-22. https://doi.org/10.1016/j.jconhyd.2016.11.001.

Christie, M., Rudolph, D.L., Payment, P., Locas, A., 2009. Monitoring the occurrence of microbial contaminants within the wellhead protection area of a municipal well field in an agricultural setting. Microbial Transport and Survival in the Subsurface: First International Conference, Niagara-on-the-Lake, ON, Canada, 10-13 May 2009.

CH2MHILL, S.S. Papadopulos & Associates Inc. (SSPA), 2003. Alder Creek Groundwater Study: Final Report. Prepared for The Regional Municipality of Waterloo, Kitchener, ON.

Collins, M., Knutti, R., Arblaster, J., Dufresne, J.-L., Fichefet, T., Friedlingstein, P., Gao, X., Gutowski Jr., W.J., Johns, T., Krinner, G., Shongwe, M., Tebaldi, C., Weaver, A.J., Wehner, M., 2013. Long-term Climate Change: Projections, Commitments and Irreversibility, in: Stocker, T.F., Qin, D., Plattner, G.-K., Tignor, M., Allen, S.K., Boschung, J., Nauels, A., Xia, Y., Bex, V., Midgley, P.M. (Eds.), Climate Change 2013: The Physical Science Basis. Contribution of Working Group I to the Fifth Assessment Report of the Intergovernmental Panel on Climate Change. Cambridge University Press, Cambridge, United Kingdom and New York, NY, USA. http://www.ipcc.ch/report/ar5/wg2/.

Cubasch, U., Meehl, G.A., Boer, G.J., Stouffer, R.J., Dix, M., Noda, A., Senior, C.A., Raper, S., Yap, K.S., 2001. Projections of Future Climate Change, in: Houghton, J.T., Ding, Y., Griggs, D.J., Noguer, M., van der Linden, P.J., Dai, X., Maskell, K., Johnson, C.A. (Eds.), Climate Change 2001: The Scientific Basis. Contribution of Working Group I to the Third Assessment Report of the Intergovernmental Panel on Climate Change. Cambridge University Press, Cambridge, UK, pp. 525-582. https://www.ipcc.ch/report/ar3/wg1/.

DHI, 2017a. MIKE SHE Volume 2: Reference guide. Hørsholm, Denmark.

DHI, 2017b. MIKE SHE Online Help Files. http://doc.mikepoweredbydhi.help/webhelp/2017/mikeshe/index.htm. (Accessed 15.05.2017).

DHI, 2017c. MIKE SHE Volume 1: User guide. Hørsholm, Denmark.

DHI-WASY, 2011. FEFLOW 6.0 – Finite Element Subsurface Flow and Transport Simulation System. WASY GmbH. Berlin, Germany.

Dingman, S.L., 2015. Physical Hydrology, 3rd ed., Waveland Press Inc., Long Grove, IL, USA.

DMTI Spatial Inc. (DMTI), 2011. CanMap Streetfiles, major water regions, and minor water regions [computer files]. University of Waterloo Geospatial Centre, controlled access. GIS digital mapping data. (Accessed 29.03.2012).

Eaton, J.W., Bateman, D., Hauberg, S., 2011. GNU Octave. Edition 3 for Octave version 3.6.4. Manual for high-level interactive language for numerical computations. https://www.gnu.org/software/octave/download.html. (Accessed 03.08.2013).

Esri, HERE, Garmin, © OpenStreetMap contributors, the GIS user community, 2019. World map. Obtained using ArcMap 10.3 software. http://goto.arcgisonline.com/maps/World_Light_Gray_Base. (Accessed 26.06.2019).

Faurès, J.-M., Goodrich, D.C., Woolhiser, D.A., Sorooshian, S., 1995. Impact of small-scale spatial rainfall variability on runoff modeling. J. Hydrol. 173, 309-326. https://doi.org/10.1016/0022-1694(95)02704-S.

Gavin, H.P., 2009. MATLAB files for the Levenberg-Marquardt algorithm for nonlinear least squares curve-fitting problems. lm.m, lm_examp.m, lm_func.m, and lm_plots.m [computer files]. CE 281: Experimental Systems course, Department of Civil and Environmental

Engineering, Duke University, Durham, NC, USA. Updated 12 Jan 2009. http://people.duke.edu/~hpgavin/ce281/. (Accessed 12.01.2019).

Gavin, H.P., 2019. The Levenberg-Marquardt algorithm for nonlinear least squares curve-fitting problems. Tutorial for CE 281: Experimental Systems course, Department of Civil and Environmental Engineering, Duke University, Durham, NC, USA. http://people.duke.edu/~hpgavin/ce281/. (Accessed 12.01.2019).

Gibbons, J.D., Chakraborti, S., 1992. Nonparametric statistical inference. 3rd ed. Marcel Dekker, New York, NY, USA. 544pp.

Government of Canada, 2013. Weather Tools – FAQ: Frequently asked questions. https://ec.gc.ca/meteo-weather/default.asp?lang=En&n=108C6C74-1#ws41070341. Date modified: 5 Jul 2013. (Accessed 19.07.2017).

Government of Canada, 2019. Historical Data: Rainfall, snowfall, and temperature data for the Roseville, ON, weather station [computer files]. http://climate.weather.gc.ca/historical_data/search_historic_data_e.html. (Accessed 18.01.2017, 05.05.2017, 07.07.2017, 15.01.2019).

Graham, D., 2017. Personal communications from senior engineer at DHI, Denmark.

Graham, D.N., Butts, M.B., 2005. Flexible integrated watershed modelling with MIKE SHE, in: Singh, V.P., Frevert, D.K. (Eds.), Watershed Models, CRC Press, Boca Raton, FL, USA, pp.245-272.

Grand River Conservation Authority (GRCA), 1998. Grand River Watershed data [computer file]. Subcatchment basins. Cambridge, Ontario: Grand River Conservation Authority. https://maps.grandriver.ca/data-gis.html. GIS digital mapping data. (Accessed 29.03.2012).

Grand River Conservation Authority (GRCA), 2017a. Daily rainfall and average temperature data from the Paris, Cambridge (Shades Mill), Baden, Burford, Laurel Creek, and Wellesley Dam climate stations [computer files]. https://data.grandriver.ca/downloads-monitoring.html. (Accessed 23.11.2017, 15.12.2017).

Grand River Conservation Authority (GRCA), 2017b. HEC2 cross-section files from "Alder Creek Floodline Mapping Study," Jan. 1997 [computer files]. Produced using information under License with the Grand River Conservation Authority. Copyright © Grand River Conservation Authority, 2017.

Healy, R.W., 2010. Estimating groundwater recharge. Cambridge University Press, Cambridge, UK.

Herschy, R.W., 1973. The magnitude of errors at flow measurements stations. Proc. of the Koblenz Symp. on Hydrometry (1970). IAHS Publ. 99, pp. 109-131. https://iahs.info/uploads/dms/099013.pdf.

Hess, T., Daccache, A., Daneshkhah, A., Knox, J., 2016. Scale impacts on spatial variability in reference evapotranspiration. Hydrol. Sci J. 61(3), 601-609. https://doi.org/10.1080/02626667.2015.1083105.

Huff, F.A., 1970. Sampling errors in measurement of mean precipitation. J. Appl. Meteorol. 9(1), 35-44. https://doi.org/10.1175/1520-0450%281970%29009%3C0035%3ASEIMOM%3E2.0.CO%3B2.

Huff, F.A., Schickedanz, P.T., 1972. Space-time uncertainties in precipitation measurement. Proc. Int. Symp. on Uncertainties in Hydrol. and Water Resour. Syst., 11-14 Dec 1972. Vol. I, 395-409. Univ. of Arizona, Tucson, AZ.

Isensee, A.R., Sadeghi, A.M., 1995. Long-term effect of tillage and rainfall on herbicide leaching to shallow groundwater. Chemosphere. 30 (4), 671-685. https://doi.org/10.1016/0045-6535(94)00433-U.

Jyrkama, M.I., Sykes, J.F., 2007. The impact of climate change on spatially varying groundwater recharge in the Grand River Watershed (Ontario). J. Hydrol. 338, 237-250. https://doi.org/10.1016/j.jhydrol.2007.02.036.

Kampf, S.K., Burges, S.J., 2010. Quantifying the water balance in a planar hillslope plot: Effects of measurement errors on flow prediction. J. Hydrol. 380, 191-202. https://doi.org/10.1016/j.jhydrol.2009.10.036.

Krajewski, W.F., Ciach, G.J., Habib, E., 2003. An analysis of small-scale rainfall variability in different climatic regions. Hydrol. Sci. J. 48(2), 151-162. https://doi.org/10.1623/hysj.48.2.151.44694.

Kristensen, K.J., Jensen, S.E., 1975. A model for estimating actual evapotranspiration from potential evapotranspiration. Nordic Hydrol. 6, 170-188. https://doi.org/10.2166/nh.1975.0012.

Leij, F.J., Alves, W.J., van Genuchten, M.Th., Williams, J.R., 1996. The UNSODA Unsaturated Soil Hydraulic Database: User's Manual Version 1.0. U.S. Environmental Protection Agency, Cincinnati, OH, USA. EPA/600/R-96/095 (NTIS 97-149496). https://cfpub.epa.gov/si/.

Linsley, R.K., Kohler, M.A., 1951. Variations in storm rainfall over small areas. Trans. Amer. Geophys. Union. 32(2), 245-250. https://doi.org/10.1029/TR032i002p00245.

Loschko, M., Wöhling, T., Rudolph, D.L., Cirpka, O.A., 2016. Cumulative relative reactivity: A concept for modeling aquifer-scale reactive transport. Water Resour. Res. 52, 8117-8137. https://doi.org/10.1002/2016WR019080.

Martin, P.J., Frind, E.O., 1998. Modeling a complex multi-aquifer system: The Waterloo Moraine. Ground Water 36(4), 679-690. https://doi.org/10.1111/j.1745-6584.1998.tb02843.x.

Matrix Solutions Inc. (Matrix), S.S. Papadopulos and Associates Inc. (SSPA), 2014a. Region of Waterloo Tier Three Water Budget and Local Area Risk Assessment, Model Calibration and Water Budget Report. Prepared for: The Regional Municipality of Waterloo. Waterloo, ON. August 2014.

Matrix Solutions Inc. (Matrix), S.S. Papadopulos and Associates Inc. (SSPA), 2014b. Region of Waterloo Tier Three Water Budget and Local Area Risk Assessment. Final Report, Sep. 2014. Prepared for: Region of Waterloo. https://www.sourcewater.ca/en/source-protection-areas/resources/Documents/Grand/RMOW-September-2014-WQRA_chpt-1-10.pdf.

Meyer, P., Martin, P., Brouwers, B., Wootton, R., Hodgins, E., 2017. Using source water protection models to manage an unexpected water supply shutdown; A case study from the

Region of Waterloo. Proc. GeoOttawa 2017: 70th Canadian Geotechnical Conference and 12th CGS/IAH-CNC Groundwater Conference, Ottawa, ON, Canada, 1-4 Oct 2017.

Mileham, L., Taylor, R., Thompson, J., Todd, M., Tindimugaya, C., 2008. Impact of rainfall distribution on the parameterization of a soil-moisture balance model of groundwater recharge in equatorial Africa. J. Hydrol. 359, 46-58. https://doi.org/10.1016/j.jhydrol.2008.06.007.

Obled, Ch., Wendling, J., Beven, K., 1994. The sensitivity of hydrological models to spatial rainfall patterns: an evaluation using observed data. J. Hydrol. 159, 305-333. https://doi.org/10.1016/0022-1694(94)90263-1.

O'Connor, D.R., 2002. Report of the Walkerton Inquiry. Part 1. The events of May 2000 and related issues. The Walkerton Inquiry, Toronto, ON. http://www.archives.gov.on.ca/en/e_records/walkerton/index.html.

Ontario Geological Survey (OGS), 2010. Surficial geology of Southern Ontario. Ontario Geological Survey, Miscellaneous Release--Data 128-REV. ISBN 978-1-4435-2482-7. Obtained from Matrix Solutions Inc., controlled access. (Accessed 29.06.2016).

Ontario Ministry of Natural Resources (OMNR), 2007. Daily weather data [computer file]. Digital Archive of Canadian Climatological Data. Obtained from Matrix Solutions Inc., controlled access. (Accessed 28.04.2016).

Ontario Ministry of Natural Resources (OMNR), 2008. Southern Ontario Land Resource Information System (SOLRIS) Land Use Data [computer files]. Obtained from University of Waterloo Geospatial Centre, Waterloo, ON, controlled access. (Accessed 03.06.2009).

Ontario Ministry of Natural Resources and Forestry (OMNRF), 2016. Watershed, Quaternary [computer file]. Revised 4 Jan 2010. https://www.ontario.ca/page/land-information-ontario. (Accessed 01.02.2017).

Paixao, E., Monirul Qader Mirza, M., Shephard, M.W., Auld, H., Klaassen, J., Smith, G., 2015. An integrated approach for identifying homogeneous regions of extreme rainfall events and estimating IDF curves in southern Ontario, Canada: Incorporating radar observations. J. Hydrol. 528, 734-750. https://doi.org/10.1016/j.jhydrol.2015.06.015.

Raes, D., 2009. The ETo Calculator: Evapotranspiration from a reference surface. Reference Manual Version 3.1. Food and Agriculture Organization of the United Nations, Land and Water Division, Rome, IT. http://www.fao.org/land-water/databases-and-software/eto-calculator/en/.

Refsgaard, J.C., Storm, B., 1995. MIKE SHE, in: Singh, V.P. (Ed.), Computer Models of Watershed Hydrology. Water Resour. Publ., Highlands Ranch, CO, USA. pp.809-846.

Region of Waterloo (ROW), 2010. Land use data for Kitchener (2010-08-31), Waterloo (2009-09-24), and Wilmot (2009-09-24) [computer files]. Region of Waterloo, Kitchener, ON. Obtained from Matrix Solutions Inc., controlled access. (Accessed 21.06.2016).

Renard, F., 2017. Local influence of south-east France topography and land cover on the distribution and characteristics of intense rainfall cells. Theor. Appl. Climatol. 128, 393-405. https://doi.org/10.1007/s00704-015-1698-1.

Rutledge, A.T., 2007. Program User Guide for PART. U.S. Geological Survey. http://water.usgs.gov/ogw/part/UserManualPART.pdf. (Accessed 17.11.2010).

Sadeghi, A.M., Isensee, A.R., 1994. Spatial distribution of atrazine residues in soil and shallow groundwater: effect of tillage and rainfall timing. Agric. Ecosyst. Environ. 48, 67-76. https://doi.org/10.1016/0167-8809(94)90076-0.

Sanderson, M.E.L., 1998. The Grand climate: weather & water in the Grand River Basin. Grand River Foundation, Cambridge, ON.

Sapriza-Azuri, G., Jódar, J., Navarro, V., Slooten, L.J., Carrera, J., Gupta, H.V., 2015. Impacts of rainfall spatial variability on hydrogeological response. Water Resour. Res. 51, 1300-1314, https://doi.org/10.1002/2014WR016168.

Schaap, M.G., Liej, F.J., van Genuchten, M. Th., 1999. A Bootstrap-neural network approach to predict soil hydraulic parameters, in: M. Th. van Genuchten, et al. (Eds.), Characterization and Measurements of the Hydraulic Properties of Unsaturated Porous Media, University of California at Riverside, Riverside, CA, USA. pp. 1237-1250.

Schuurmans, J.M., Bierkens, M.P.F., 2007. Effect of spatial distribution of daily rainfall on interior catchment response of a distributed hydrological model. Hydrol. Earth Sys. Sci. 11, 677-693. https://doi.org/10.5194/hess-11-677-2007.

Scurlock, J.M.O., Asner, G.P., Gower, S.T., 2001. Worldwide Historical Estimates of Leaf Area Index, 1932-2000. ORNL Tech. Memo. TM-2001/268. Oak Ridge National Laboratory, Oak Ridge, TN, USA. https://doi.org/10.2172/814100.

Shifflett, S., 2018. Personal communications from water resources engineer, Grand River Conservation Authority.

Singh, V.P., 1992. Elementary Hydrology. Prentice Hall, Englewood Cliffs, NJ, USA.

Sousa, M.R., Frind, E.O., Rudolph, D.L., 2013. An integrated approach for addressing uncertainty in the delineation of groundwater management areas. J. Contam. Hydrol. 148, 12-24. https://doi.org/10.1016/j.jconhyd.2013.02.004.

Sousa, M.R., Jones, J.P., Frind, E.O., Rudolph, D.L., 2013. A simple method to assess unsaturated zone time lag in the travel time from ground surface to receptor. J. Contam. Hydrol. 144(1), 138-151. https://doi.org/10.1016/j.jconhyd.2012.10.007.

Thodal, C.E., 1997. Hydrogeology of Lake Tahoe Basin, California and Nevada, and results of a ground-water quality monitoring network, water years 1990–92. U.S. Geological Survey Water-Resour. Inv. Rep. 97-4072. https://pubs.usgs.gov/wri/1997/4072/report.pdf.

Tsanis, I.K., Gad, M.A., 2001. A GIS precipitation method for analysis of storm kinematics. Environ. Modell. Softw. 16, 273-281. https://doi.org/10.1016/S1364-8152(00)00068-2.

Villarini, G., Mandapaka, P.V., Krajewski, W.F., Moore, R.J., 2008. Rainfall and sampling uncertainties: A rain gauge perspective. J. Geophys. Res. 113, D11102. https://doi.org/10.1029/2007JD009214.

Villarini, G., Smith, J.A., Baeck, M.L., Sturdevant-Rees, P., Krajewski, W.F., 2010. Radar analyses of extreme rainfall and flooding in urban drainage basins. J. Hydrol. 381, 266-286. https://doi.org/10.1016/j.jhydrol.2009.11.048.

Water Survey of Canada (WSC), 2017. Archived hydrometric data: Daily discharge data for Alder Creek near New Dundee [computer files]. http://wateroffice.ec.gc.ca/index_e.html. (Accessed 13.07.2017).

Wiebe, A.J., Conant Jr., B., Rudolph, D.L., Korkka-Niemi, K., 2015. An approach to improve direct runoff estimates and reduce uncertainty in the calculated groundwater component in water balances of large lakes. J. Hydrol. 531, 655-670. https://doi.org/10.1016/j.jhydrol.2015.10.061.

Wiebe, A.J., Menkveld, P.G., Hillier, C.E., Mesec, E., Rudolph, D.L., 2019. Meteorological and hydrological data from the Alder Creek watershed, Grand River basin, Ontario. https://doi.org/10.20383/101.0178.

Winter, T.C., 1981. Uncertainties in estimating the water balance of lakes. Water Resour. Bull. 17(1), 82-115. https://doi.org/10.1111/j.1752-1688.1981.tb02593.x.

Yin, Y., Sykes, J.F., Normani, S.D., 2015. Impacts of spatial and temporal recharge on field-scale contaminant transport model calibration. J. Hydrol. 527, 77-87. https://doi.org/10.1016/j.jhydrol.2015.04.040.

Zhao, F., Zhang, L., Chiew, F.H.S., Vaze, J., Cheng, L., 2013. The effect of spatial rainfall variability on water balance modelling for south-eastern Australian catchments. J. Hydrol. 493, 16-29. https://doi.org/10.1016/j.jhydrol.2013.04.028.

Tables

Table 1. Annual rainfall* (mm) recorded at stations of the local, regional, and national networks.

	Rainfall		
Weather Station	2014	2015	2016
WS2	987	839	371
WS3	794	784	797
WS4	892	853	665
WS5	N/A†	725	746
WS6‡	800	927	414
WS7	560	673	789
Wellesley§	849	690	888
Baden§	731	626	537
Laurel Creek§	701	612	605
Cambridge§	677	464	747
Paris§	597	759	892
Burford§	432	641	329
Roseville** (755)	665	689	746

* Snowfall data are not included. Roseville snowfall amounts were 183 mm, 111 mm, and 153 mm for 2014, 2015, and 2016, respectively (Government of Canada, 2019).

† N/A – not available. WS5 data collection started in June 2014. Jun to Dec 2014: 600 mm.

‡ The rainfall time series at WS6 is a composite from two gauges at this station.

§ Grand River Conservation Authority weather station (GRCA, 2017a).

** Environment Canada Weather station (Government of Canada, 2019). The amount in brackets is the average rainfall from 1973 to 2018.

Table 2. Unsaturated soil properties (D. Graham, pers. comm., 2017; Leij et al., 1996; Schaap et al., 1999; Sousa, Jones, et al., 2013).

Soil Unit	K_{sat}* (m/s)	θ_{sat}** (-)	θ_{res}*** (-)	n† (-)	α†† (cm^{-1})
Outwash gravel	$5x10^{-4}$	0.28	0.04	4.0	0.040
Ice-contact gravel	$3x10^{-4}$	0.33	0.04	3.3	0.040
Outwash sand	$6.5x10^{-5}$	0.43	0.05	3.2	0.035
Ice-contact sand	$7x10^{-5}$	0.35	0.05	3.3	0.035
Bog/swamp deposits	$1x10^{-5}$	0.60	0.20	3.0	0.030
Stream alluvium	$1x10^{-6}$	0.41	0.07	1.5	0.010
Port Stanley Till	$5x10^{-6}$	0.40	0.06	1.5	0.020
Maryhill Till	$1x10^{-6}$	0.45	0.06	1.2	0.021
Lacustrine deposits	$1x10^{-6}$	0.45	0.09	1.3	0.020

* K_{sat} = saturated hydraulic conductivity

** θ_{sat} = saturated moisture content

*** θ_{res} = residual moisture content

† n = van Genuchten fitting parameter

†† α = inverse air entry pressure for van Genuchten curve

Table 3. Fitting parameters for the spatial correlation best-fit curves.

Network	Method	Time scale	Nugget (c_1; -)	Correlation Distance (c_2; km)	Shape Factor (c_3; -)
Local with Regional	Spearman	1 hr	1.0	88.4	0.21
		3 hr	1.0	113.3	0.24
		24 hr	1.0	91.2	0.39
		1 month	1.0	87.5	0.27

Table 4. Numerical model water budget results and comparisons (results in mm per m^2 per yr).

Year	Component	Scenario		
		1	2	3
2014	Precipitation	849	895	1048
	Evapotranspiration[*]	392	376	381
	Overland Runoff[†]	91	96	124
	Storage change[‡]	-53	-33	-20
	Recharge[§]	421	456	562
	Streamflow at node representing WSC gauge[**]	107	112	148
	Total Streamflow[††]	121	127	157
2015	Precipitation	789	714	897
	Evapotranspiration[*]	425	421	428
	Overland Runoff[†]	68	61	85
	Storage change[‡]	7	-9	20
	Recharge[§]	288	241	364
	Streamflow at node representing WSC gauge[**]	84	75	101
	Total Streamflow[††]	97	88	116
2016	Precipitation	879	756	771
	Evapotranspiration[*]	444	382	338
	Overland Runoff[†]	78	64	93
	Storage change[‡]	13	25	-10
	Recharge[§]	344	285	349
	Streamflow at node representing WSC gauge[**]	96	79	112
	Total Streamflow[††]	107	91	122
Recharge Estimate from Previous Study (Tier Three[‡‡])		321		
Streamflow estimates from WSC gauge[§§]	2014	153		
	2015	112		
	2016	135		

* AET excluding AET from the saturated zone. Total AET values were: 493, 476, and 496 mm for Scenarios 1 to 3 for 2014; 521, 505, and 533 mm, respectively, for 2015; and 540, 466, and 439 mm, respectively, for 2016.

† Overland flow into stream.

‡ Includes storage change (unsaturated, snow, and overland flow zones), and boundary flows out of the unsaturated zone (~5 mm/yr/scenario). Boundary flows into the unsaturated zone: 0 mm.

§ Recharge can be calculated via Eqn. (3).

** Area above gauge = 47.4 km^2 (WSC, 2017).

†† Area of model domain = 68.2 km^2 (GRCA, 1998).

‡‡ Annual results from calibrated, steady state, saturated zone FEFLOW simulation for Regional Municipality of Waterloo Tier Three Assessment (M.H. Brouwers, pers. comm., 2017; Matrix and SSPA, 2014a).

§§ WSC (2017). The sums here are based on the 52-week periods of the simulations. There were twelve days with missing data at the start of 2016.

Figures

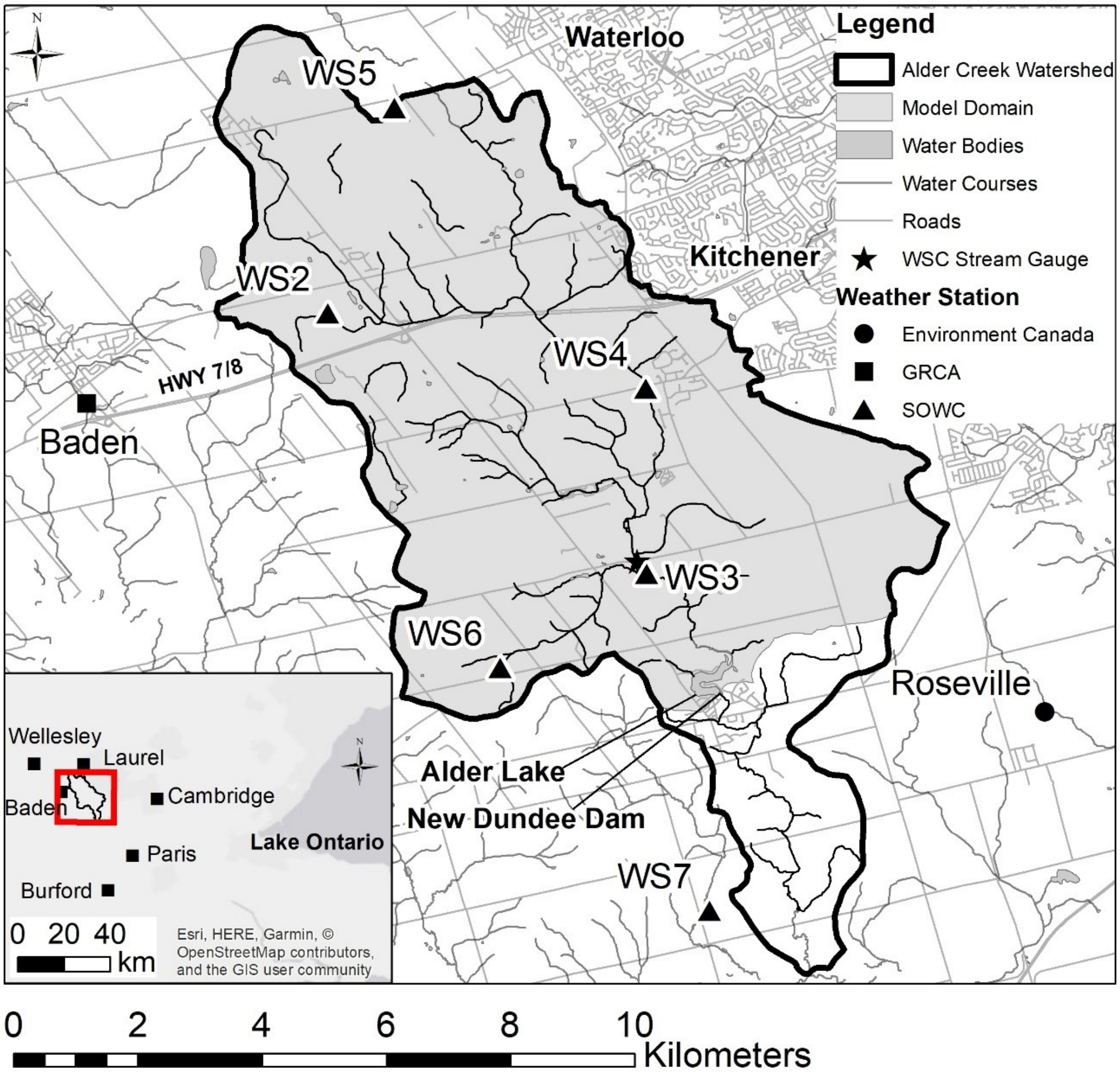

Figure 1: The Alder Creek watershed, with Environment Canada, GRCA, and SOWC weather station locations (DMTI, 2011; Esri et al., 2019; Government of Canada, 2019; GRCA, 1998, 2017a; WSC, 2017). The Water Survey of Canada (WSC) stream gauging station location is also shown near WS3.

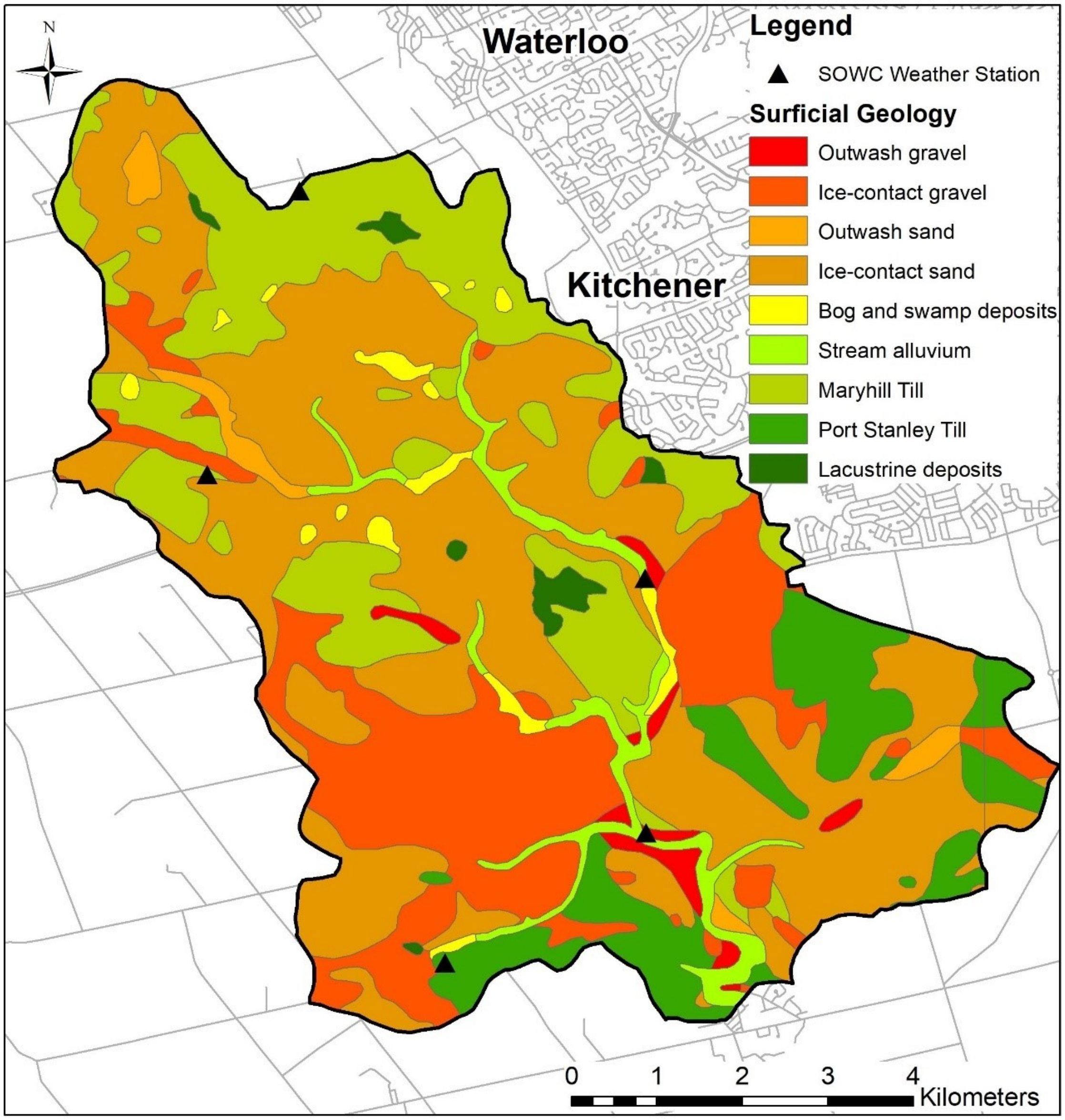

Figure 2: Surficial soils in the model domain (DMTI, 2011; GRCA, 1998; OGS, 2010).

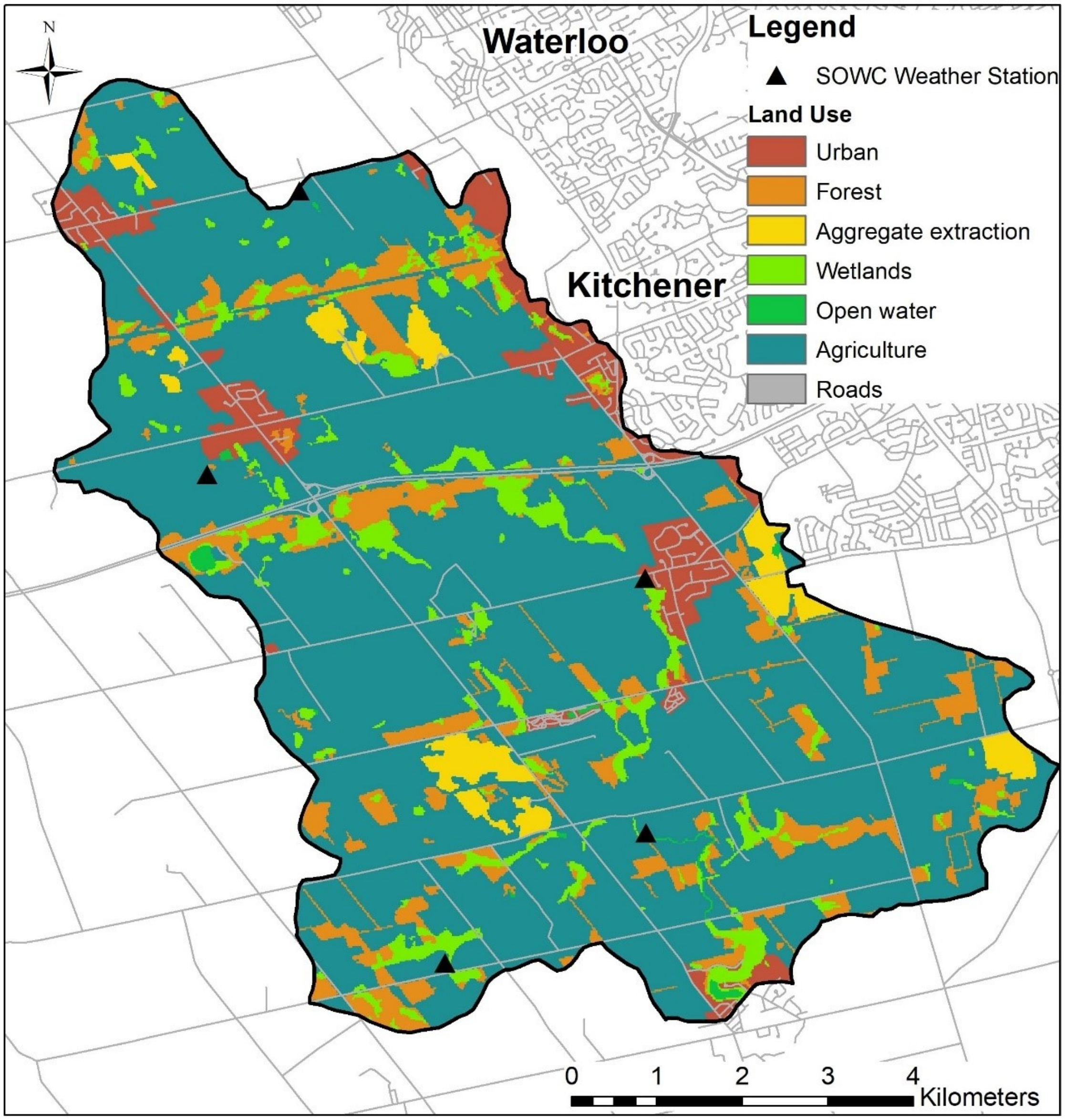

Figure 3: Land use in the model domain (DMTI, 2011; GRCA, 1998; OMNR, 2008; ROW, 2010). The "Agriculture" category includes minor areas of recreation and open land.

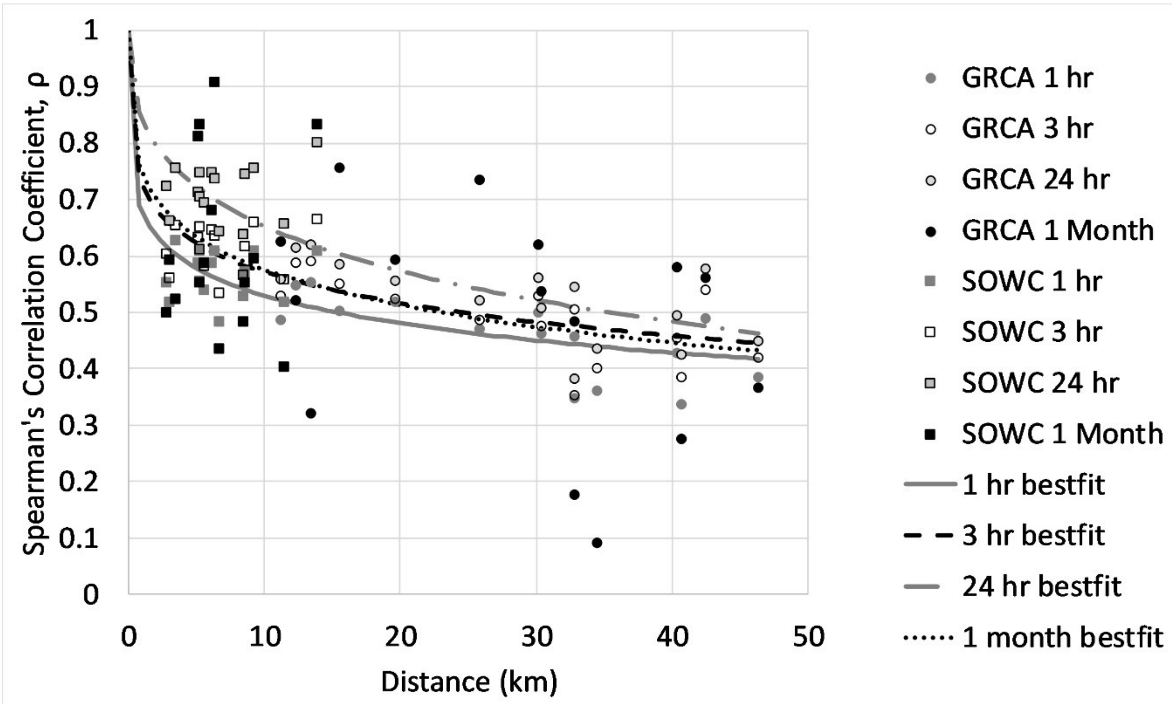

Figure 4: Spatial correlation between rainfall measurements for the combined stations of the local and regional networks.

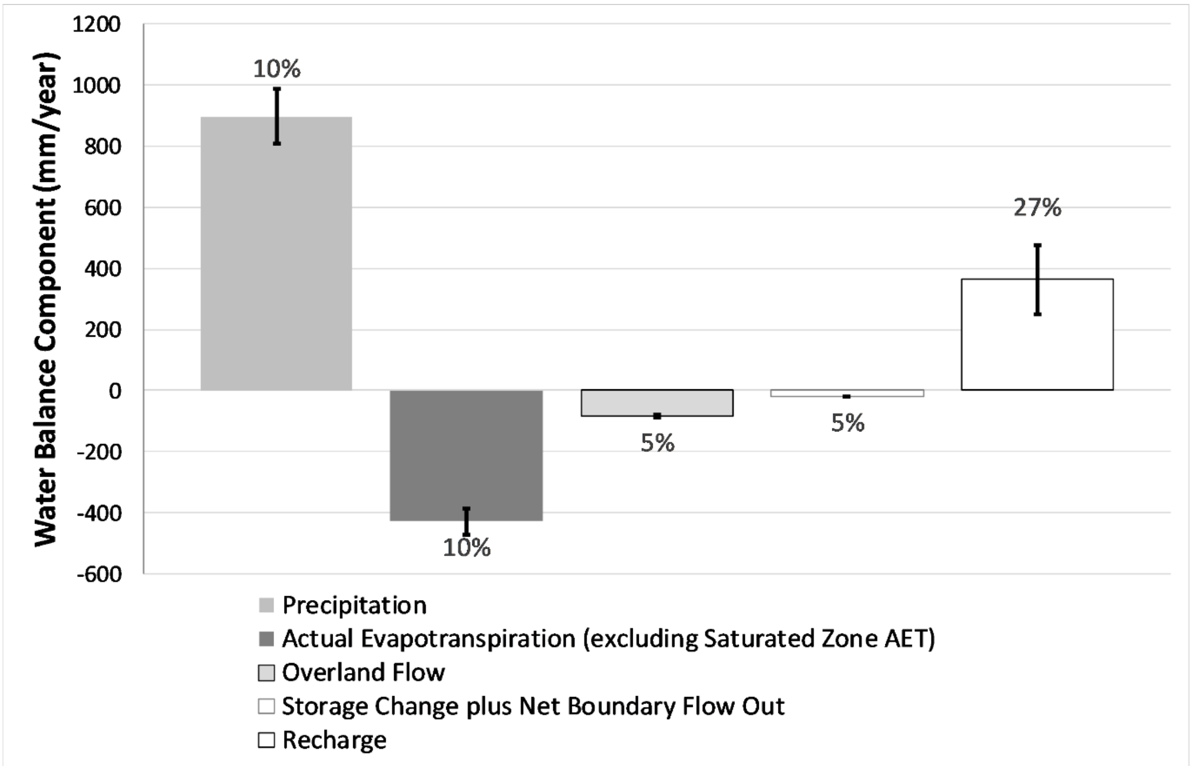

Figure 5: Instrument and method uncertainty for the Scenario 3 (2015) overall, near-surface water budget.

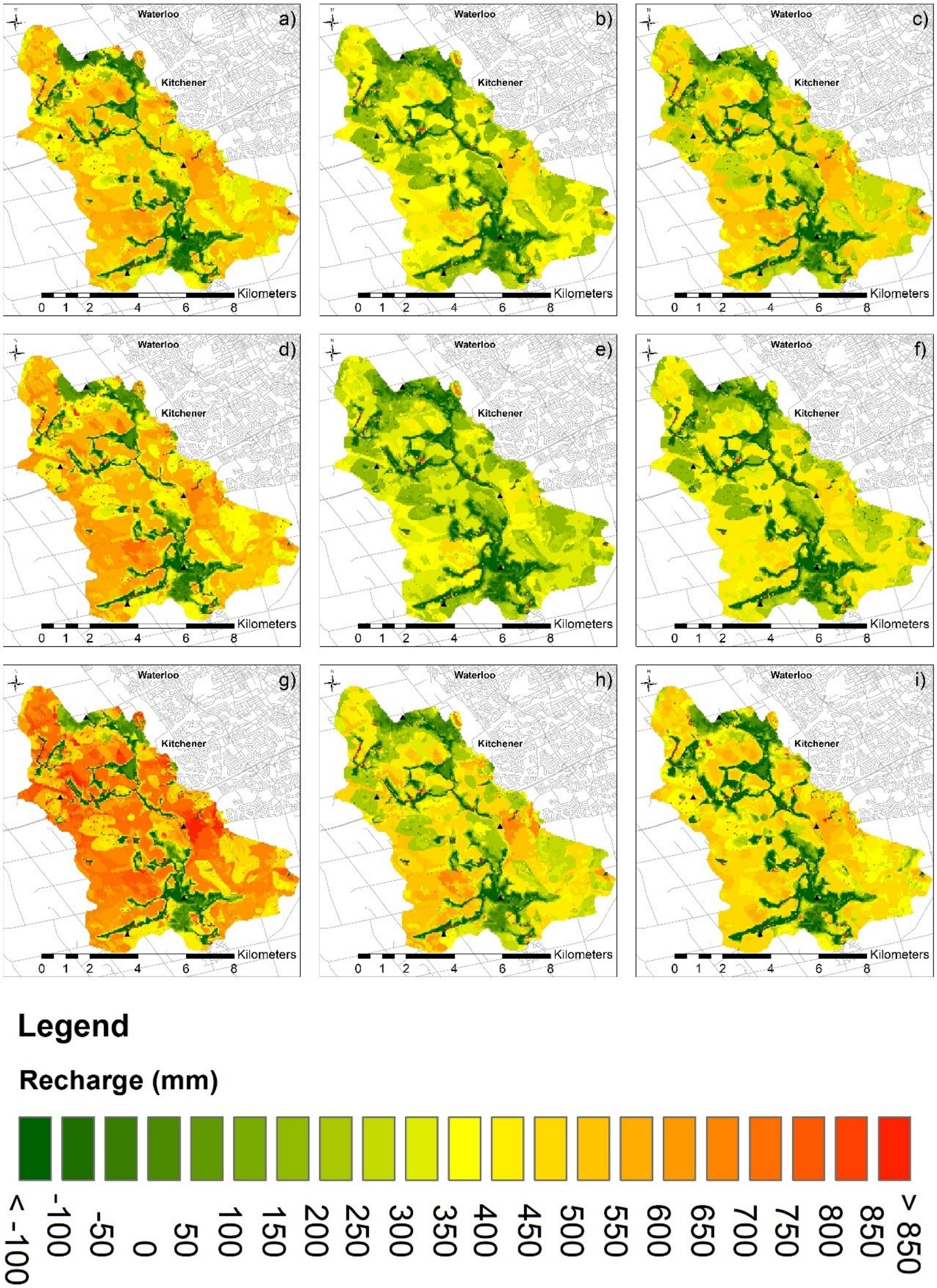

Figure 6: Recharge estimates for the three rainfall scenarios (GRCA, 1998; DMTI, 2011). Maps show results as follows: Scenario 1 (national), (a) 2014, (b) 2015, and (c) 2016; Scenario 2 (regional), (d) 2014, (e) 2015, and (f) 2016; and Scenario 3 (local), (g) 2014, (h) 2015, and (i) 2016. The local weather stations are shown as black triangles.

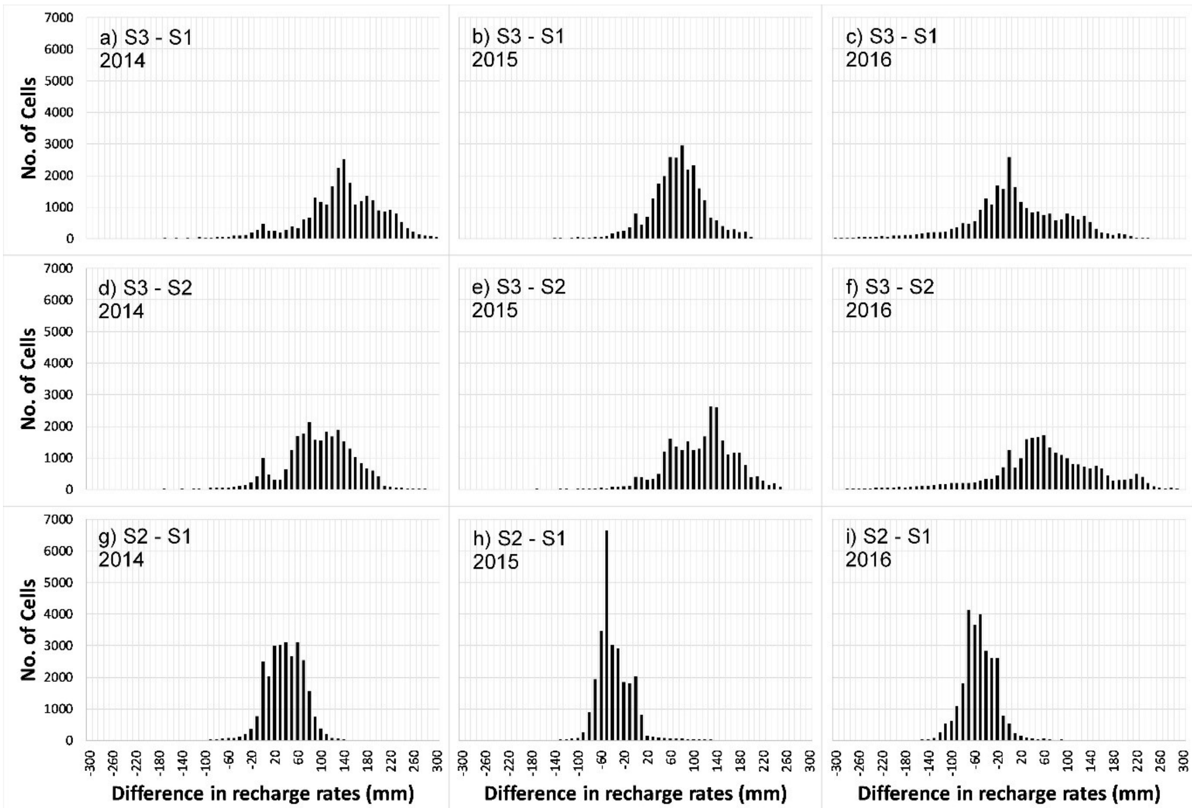

Figure 7: Frequency of differences in recharge rates between the three rainfall scenarios. "S3 - S1" implies a cell-by-cell subtraction of Scenario 1 from Scenario 3, etc.

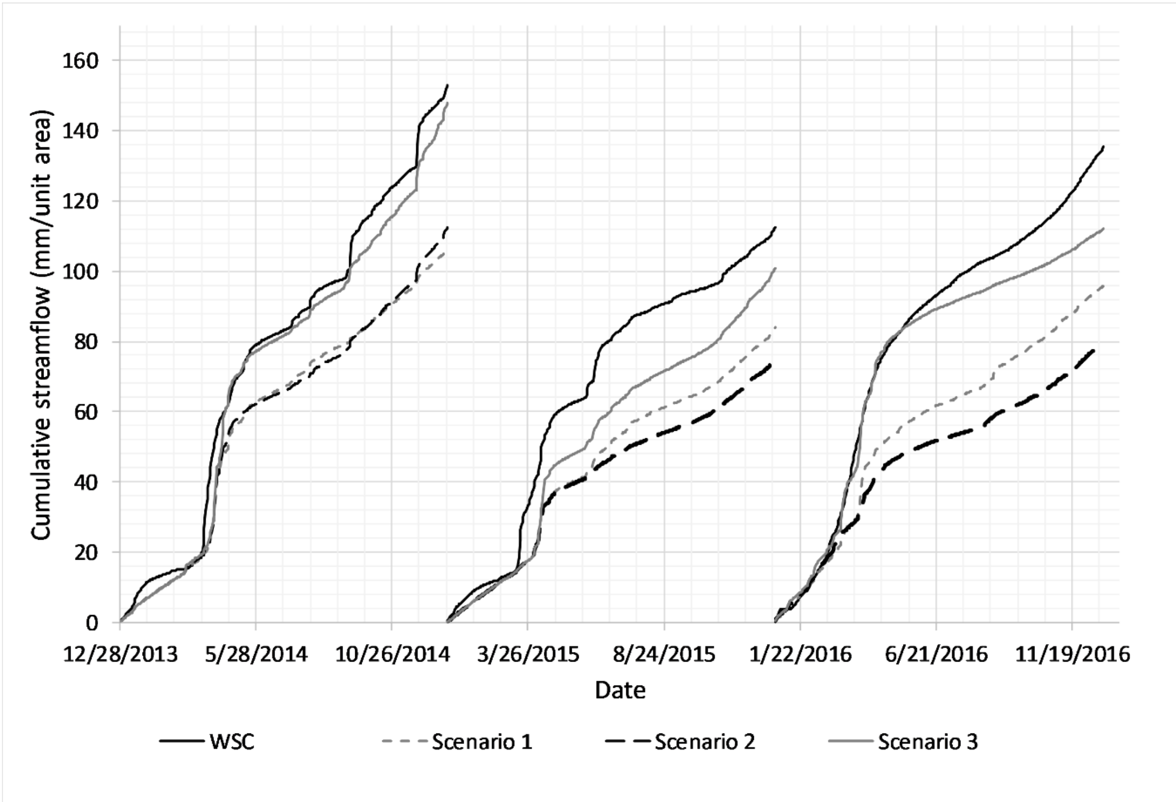

Figure 8: Comparison of cumulative streamflow results for the three simulations with recorded flows at the Water Survey of Canada (WSC) gauge. The WSC gauge was missing 12 days of data at the start of 2016.

Appendix A: Supplementary information

This supplementary information file contains: a brief description of one additional model scenario, examples of the interpolated rainfall distributions, and a comparison of observed and modelled rainfall frequency distributions.

One scenario was considered in addition to the national, regional, and local rainfall scenarios presented. This scenario was conceptualized as a reference scenario in which rainfall was interpolated from the set of all thirteen available rain gauges (Table 1). Interpolations were made at the daily time scale using the inverse distance squared method.

Figure A.1 suggests that the reference scenario results were very similar to those of the local scenario for several larger rainfall events and contain only minor differences. Table A.1 shows the individual stations' readings for these examples. The cumulative streamflow results of the reference scenario were similar to (within about 20 mm per unit area of) the cumulative streamflow results of the regional and national scenarios in 2014, and very similar to (within a few mm per unit area of) those from the local rainfall scenario in 2015 and 2016 (Figure A.2). Results for the water balance components of the reference scenario were intermediate values between the local and regional scenarios' results, but the values were generally closer to the local scenario. This is likely because of the immediate impacts of the local gauges within the watershed through the interpolated precipitation distribution. The minimal differences between the reference scenario and the local rainfall scenario, and the poorer match between the reference scenario and the observed streamflow results suggest that this reference scenario does not constitute an improvement with respect to the results of the local scenario.

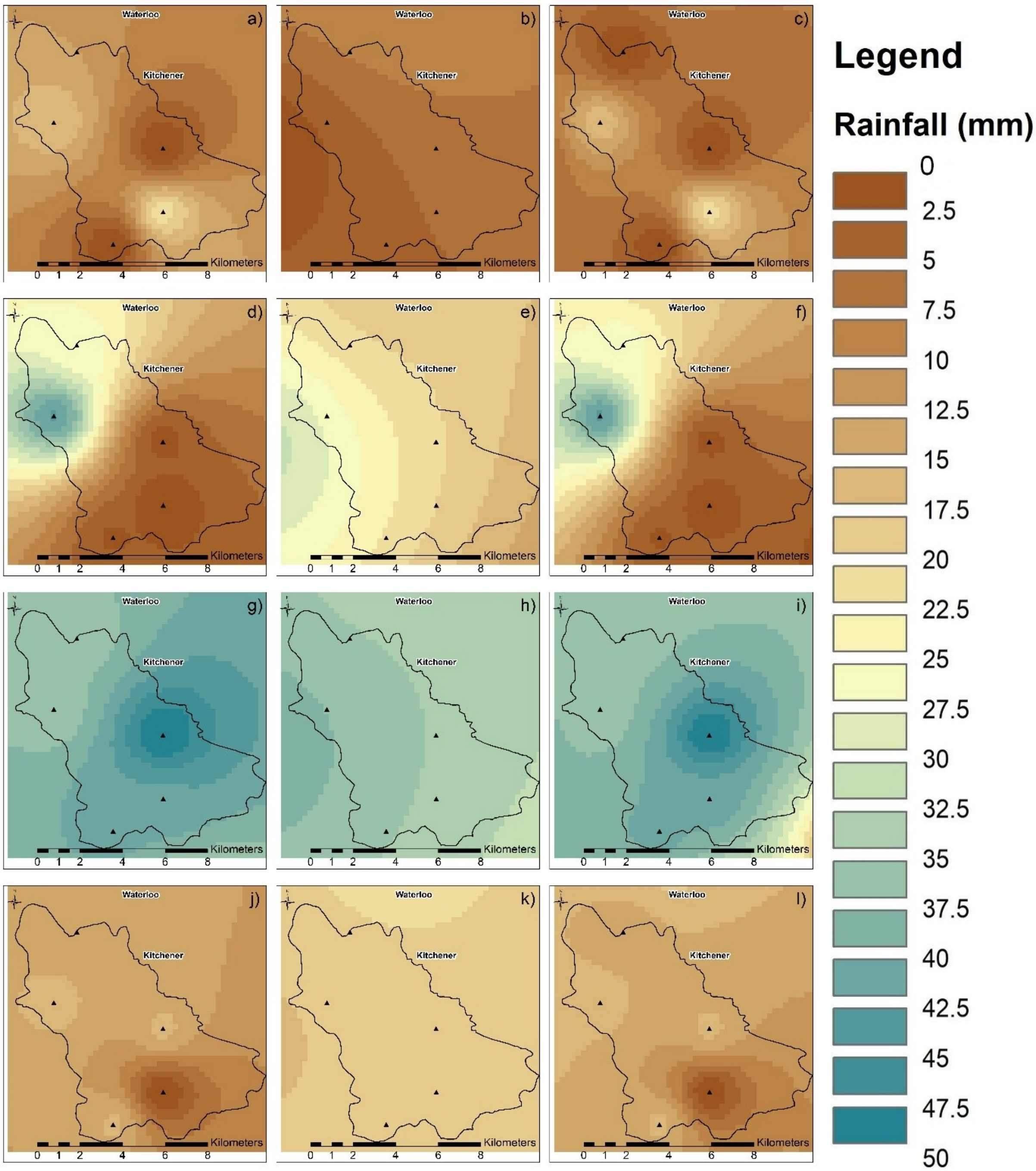

Figure A.1: Examples of rainfall interpolations for 20 May 2014 (a, b, c), 15 Jul 2014 (d, e, f), 24 Nov 2014 (g, h, i), and 20 Apr 2015 (j, k, l). The first column (a, d, g, j) shows results for the local network, the second column (b, e, h, k) shows results for the regional network, and the third column (c, f, i, l) shows results for the reference scenario (all networks).

Table A.1. Daily rainfall (mm) on the four days portrayed in Figure A.1 (GRCA, 2017a; Government of Canada, 2019).

	Rainfall			
Weather Station	**20-May-14**	**15-Jul-14**	**24-Nov-14**	**20-Apr-15**
WS2	16.8	42.8	35.6	15.8
WS3	21.2	0.0	42	0
WS4	0.0	1.6	50.2	15.6
WS5	N/A	26.0	35.8	14
WS6	0.0	2.2	41	15.4
WS7	15.2	0.6	25.6	11
Wellesley	22	14.6	34.2	17.2
Baden	0	31.4	39.2	17.2
Laurel	10	18.6	34.4	20.8
Cambridge	6.2	0.4	26.2	14.4
Paris	0.8	0.6	25.6	22.8
Burford	0	0.6	20.4	19
Roseville	15.2	0	3.7	0.6

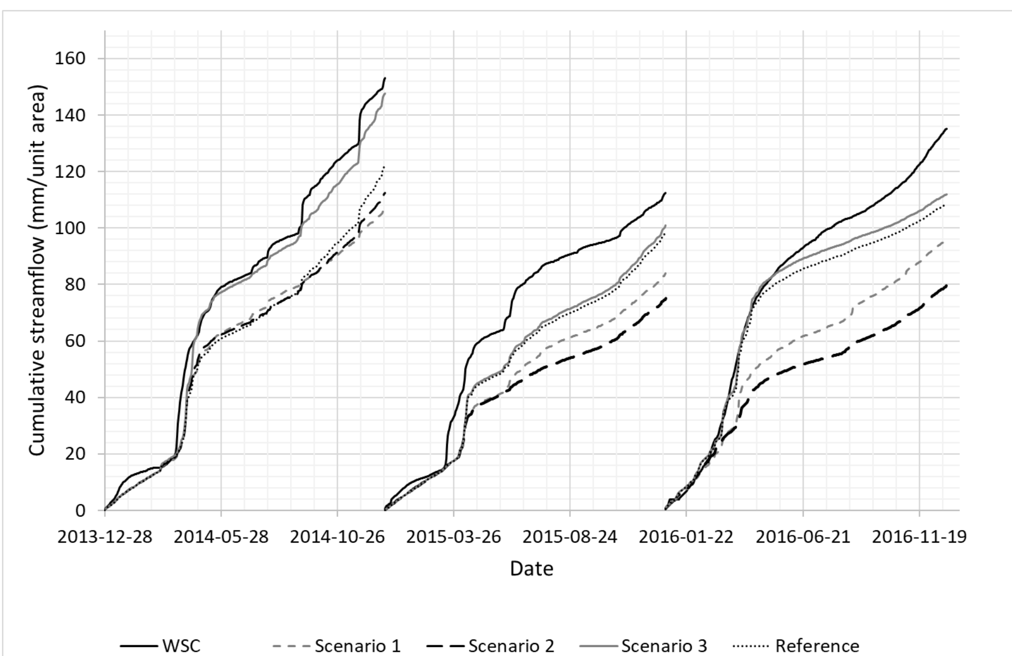

Figure A.2: Cumulative streamflow results from all scenarios including the reference scenario.

Figure A.3 shows the simulated and observed rainfall frequencies for depths less than 20 mm. The simulated frequencies tend to be similar or slightly higher than the observed regional and local values. The simulated frequencies follow the same pattern as the local and regional frequencies, unlike what was observed during spatial rainfall distribution analysis by Mileham et al. (2008), where the simulated and observed frequency patterns differed to a greater extent.

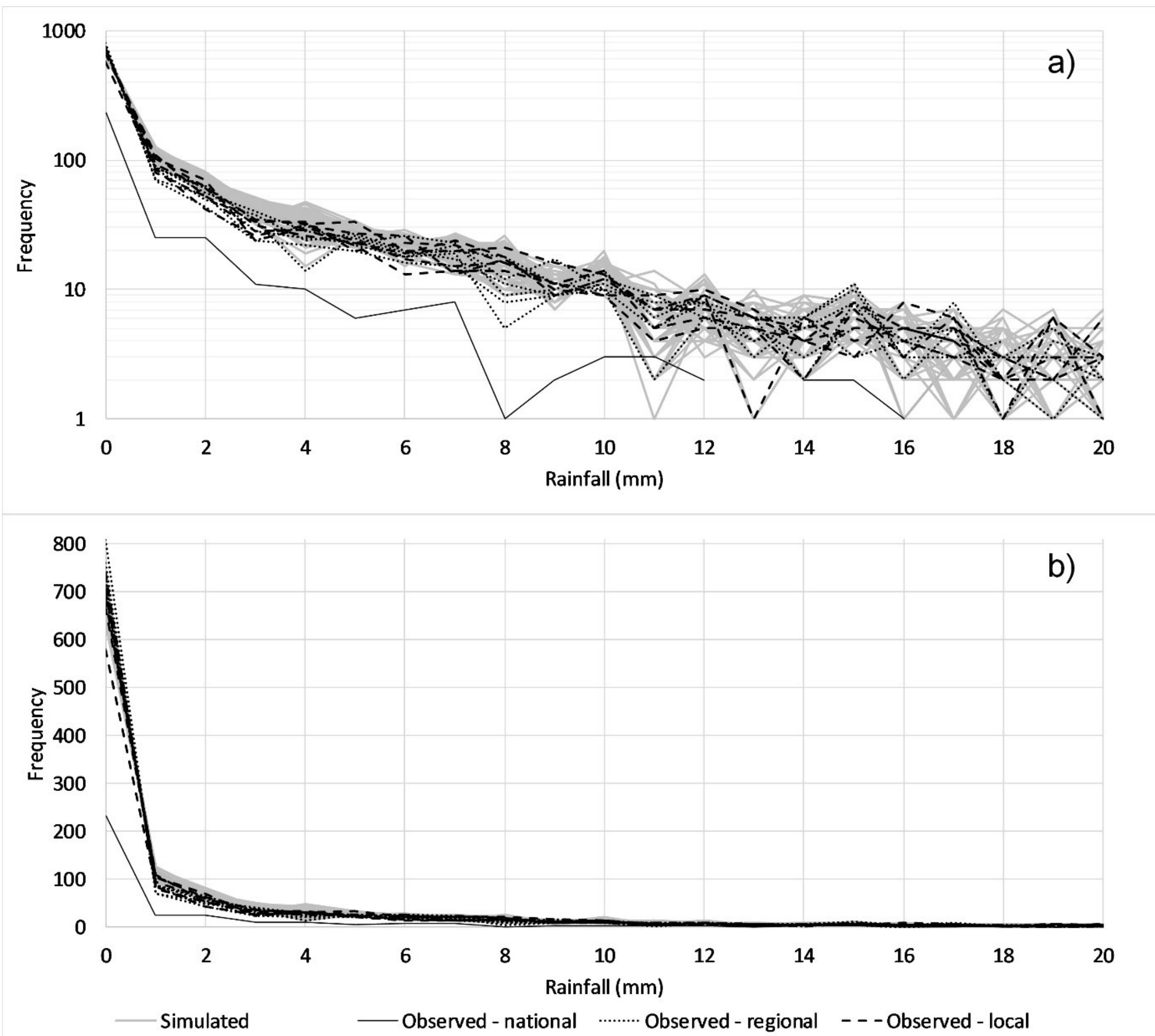

Figure A.3: Frequency distributions of observed and simulated daily rainfall: a) log scale for frequency, b) linear scale for frequency (Government of Canada, 2019; OMNR, 2007; GRCA, 2017a; Wiebe et al., 2019). The simulated rainfall time series were extracted from 36 grid cells for both the regional and local rainfall scenarios.